

Modelling and Simulation of Temporomandibular Joints with Temporomandibular Dysfunction for Orthosis Development

Modellierung und Simulation von Kiefergelenken bei Temporomandibulären Dysfunktionen zur Orthesenentwicklung

Bachelor thesis by Laura Jehn

Date of submission: 11. Mai 2021

1. Review: Prof. Dr. Oskar von Stryk
2. Review: Dr.-Ing. Jérôme Kirchhoff
Darmstadt



TECHNISCHE
UNIVERSITÄT
DARMSTADT



Computer Science
Department
Fachgebiet Simulation,
Systemoptimierung und
Robotik

Modelling and Simulation of Temporomandibular Joints with Temporomandibular Dysfunction for
Orthosis Development
Modellierung und Simulation von Kiefergelenken bei Temporomandibulären Dysfunktionen zur
Orthesenentwicklung

Bachelor thesis by Laura Jehn

1. Review: Prof. Dr. Oskar von Stryk
2. Review: Dr.-Ing. Jérôme Kirchhoff

Date of submission: 11. Mai 2021

Darmstadt

Erklärung zur Abschlussarbeit gemäß §22 Abs. 7 und §23 Abs. 7 APB der TU Darmstadt

Hiermit versichere ich, Laura Jehn, die vorliegende Bachelorarbeit ohne Hilfe Dritter und nur mit den angegebenen Quellen und Hilfsmitteln angefertigt zu haben. Alle Stellen, die Quellen entnommen wurden, sind als solche kenntlich gemacht worden. Diese Arbeit hat in gleicher oder ähnlicher Form noch keiner Prüfungsbehörde vorgelegen.

Mir ist bekannt, dass im Fall eines Plagiats (§38 Abs. 2 APB) ein Täuschungsversuch vorliegt, der dazu führt, dass die Arbeit mit 5,0 bewertet und damit ein Prüfungsversuch verbraucht wird. Abschlussarbeiten dürfen nur einmal wiederholt werden.

Bei der abgegebenen Thesis stimmen die schriftliche und die zur Archivierung eingereichte elektronische Fassung gemäß §23 Abs. 7 APB überein.

Bei einer Thesis des Fachbereichs Architektur entspricht die eingereichte elektronische Fassung dem vorgestellten Modell und den vorgelegten Plänen.

Darmstadt, 11. Mai 2021

L. Jehn

Abstract

Temporomandibular disorder (TMD) is a common disorder involving the temporomandibular joint (TMJ), the masticatory muscles and associated head and neck musculoskeletal structures, often resulting in a limited range of motion of the jaw. Treatment options are diverse, ranging from resting the jaw to manually exercising the jaw muscles, but treatment effectiveness is limited. To improve treatment options for patients suffering from TMD, this research seeks to provide the framework for a new kind of orthosis, which will allow personalised treatment for a variety of symptoms, enable jaw rehabilitation in all movement directions, and track the patients' progress over time.

For this purpose, a personalisable biomechanical jaw model was developed based on an existing model of a healthy jaw. In this model, the condylar slope can be personalised to the patient, and the maximum bite force and range of motion of the model fitted to that of the patient, enabling the development of personalised therapy routines. Resistance training and trajectory following therapy routines were implemented, and could be realised with the orthosis. The developed framework consists of a kinematic model for describing the range of motion of the orthosis, and the translation of external forces, acting on the jaw as part of a therapy routine, to orthosis actuation. In principal, this allows for an evaluation of the effectiveness of the orthosis during its development. The system offers the possibility to develop further therapy routines with little effort, allowing the capabilities of the orthosis to be continuously and easily expanded.

Contents

1. Introduction	1
2. Foundations	3
2.1. Biomechanics of the TMJ	3
2.2. Kinematics of the mandible	5
3. Related Work	6
3.1. Jaw rehabilitation devices	6
3.1.1. Insertion based devices	6
3.1.2. 6-DOF Parallel Robot	7
3.1.3. A Novel Automated Device	7
3.1.4. Exoskeleton	8
3.2. Biomechanic modelling of the jaw	9
3.3. Kinematic modelling of mandibular movement	11
3.3.1. Revolute joints	11
3.3.2. Non-orthogonal floating axis joint coordinate system	12
3.3.3. Higher kinematic pair TMJ	13
3.3.4. Instantaneous centre of rotation	14
3.4. Conclusion	15
4. Jaw Modelling	17
4.1. The biomechanical model	17
4.2. Personalising the model	18
4.2.1. Articular disk	18
4.2.2. Condylar slope	19
4.3. Modelling TMD	22
4.3.1. Limited range of motion	22
4.3.2. Reduced bite force	24
4.4. Conclusion	25
5. Orthosis Development	26
5.1. Kinematic model	26
5.1.1. Forward kinematics	27
5.1.2. Parameter boundaries	28
5.1.3. Inverse kinematics	30

5.1.4. Torque calculation	31
5.2. Therapy routines	31
5.2.1. Trajectory following	32
5.2.2. Resistance training	32
5.3. Conclusion	33
6. Evaluation	35
6.1. Evaluation of the kinematic model	35
6.1.1. Mouth opening	36
6.1.2. Mastication	37
6.1.3. Torque calculation	38
6.2. Evaluation of the trajectory following	40
6.3. Evaluation of the resistance training	42
6.4. Conclusion	45
7. Conclusion and Future Work	46
Bibliography	47
A. Appendix	50
List of Figures	52
List of Tables	53
A.1. Code structure	54
A.2. Interfacing ArtiSynth with Jython	55
A.2.1. Basics	55
A.2.2. Setting control parameters for trajectory following	55
A.2.3. Setting mode for resistance training	56
A.3. Output probes	57
A.3.1. Mouth opening distance	57
A.3.2. Mouth opening angle	57
A.4. FEM modelling of the articular disk	58
A.4.1. Code	58
A.4.2. Difficulties	62

1. Introduction

Temporomandibular disorder (TMD) is a very common disorder involving the temporomandibular joint (TMJ), the masticatory muscles and associated head and neck musculoskeletal structures. The disorder is described in [1] and will be summarised in this paragraph. TMD includes displacement disorders due to misalignment of the jaw, displacement of the articular disk, degenerative joint disease and myofascial pain disorder, the latter being the most common. While 5 to 60% of the population show at least one sign of TMD, only 5 to 10% of those with symptoms require treatment. The condition is especially prevalent among women of the ages 25-45 and patients frequently present with impaired muscle function, limited or asymmetric mandibular motion, pain or discomfort in the muscles and TMJ noises during jaw movement. In some cases, patients even have a “lockjaw”, meaning that they cannot open their mouth at all anymore.

The cause for TMD is considered multifactorial and has not been fully understood, therefore treatment is complicated and mostly focuses on treating symptoms like alleviating pain or increasing the range of motion of the mandible. In less severe cases, treatment can consist of resting the jaw, applying heat or taking muscle relaxants, all designed to reduce increased muscle activity and in turn alleviate pain. Beyond that, a wide range of jaw appliances exists that focus on altering joint mechanics, here, the oral splint for example is very common. Moreover, for increasing the range of motion of the mandible and recovering muscle ability, exercising the jaw muscles is also very effective [2] and there are many supporting devices designed for this purpose, including robotic devices that perform exercises like chewing and jaw opening. There are many treatment options, but because there are so many different forms of the disorder and the pathology is highly individual, treatment has to be personalised as well.

To explore treatment options, the dynamics of the jaw and especially the temporomandibular joint have to be well understood. Jaw biomechanics are very complex and it is complicated to measure muscle activation or joint loads in a living patient. In vivo joint force measurements are not directly possible because of the small size and complex organisation of the joint. As a result, research in this area is limited. However, several imaging techniques are available (MRI, CT, ultrasonography) and support biomechanical modelling of the jaw. Computer simulations of the jaw have thus become important as one of the few means to investigate this complex system. Biomechanical models of the jaw already exist, however, they have to be adapted to the patient’s individual anatomy and dysfunctions in the jaw. This is important for personalised treatment planning and to be able to better predict the outcome of these treatments and how they affect jaw dynamics.

Based on such a model, an active, intelligent orthosis can be developed and therapy routines evaluated in simulation. The biomechanical model can be used to investigate how an orthosis can reduce

dysfunction or joint loading and aid in performing tasks like chewing and jaw opening and help with orthosis design. Since there are many forms of the disorder, any design that seeks to be of broad use for the treatment of TMD needs to be personalisable and include a wide variety of treatment approaches.

This research aims to create the basis for the development of an active, intelligent orthosis, addressing the limitations in existing therapeutic devices for the treatment of TMD. Such an orthosis should help a patient regain full jaw movement range, support them during the rehabilitation and allow the analysis of jaw dynamics. In this context, the goal is to:

- provide a personalisable biomechanical jaw model based on an existing model of a healthy jaw,
- define the range of motion of the orthosis with the help of a kinematic model,
- develop and simulate therapy routines with the jaw model,
- relate external forces acting on the jaw as part of a therapy routine to orthosis actuation.

Jaw and temporomandibular joint anatomy and function will be explained in Chapter 2.

An overview of existing jaw rehabilitation devices, biomechanical jaw models and mathematical models for describing mandibular motion can be found in Chapter 3.

In Chapter 4, a biomechanical jaw model and methods for personalising the model and modelling TMD will be presented.

Chapter 5 elaborates the orthosis development, including the specification of the range of motion of the orthosis and application of the orthosis for therapy routines.

In Chapter 6, the orthosis framework, specifically the kinematic model and its application to therapy routines, is evaluated and Chapter 7 concludes the thesis.

2. Foundations

In this chapter, an introduction will be given to the biomechanics of the temporomandibular joint (TMJ) and the kinematics of the mandible. These are important aspects to understand and consider for jaw modelling and orthosis development.

2.1. Biomechanics of the TMJ

The temporomandibular joint is the most used joint in our body, as it is needed constantly for chewing and speaking.

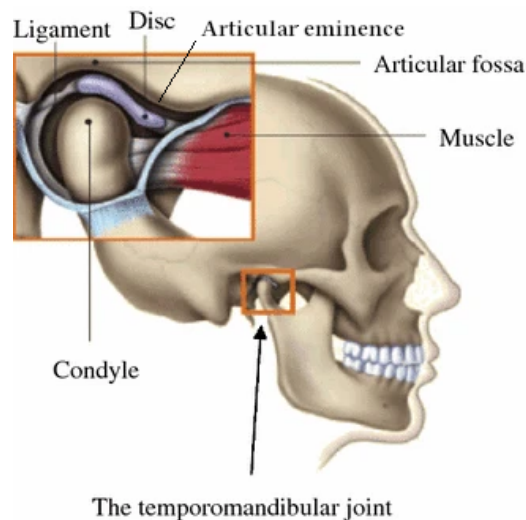


Figure 2.1.: Anatomy of the TMJ. Adopted from [3].

In Figure 2.1 the anatomy of the temporomandibular joint is depicted. The TMJ connects the upper and lower jaw, in other words, the maxilla and the mandible, and mainly consists of the condyle and the articular fossa. The condyle is the spherical, upper part of the mandible and lies inside the curvature of the articular fossa if the mouth is closed. Both, the articular disc and articular cartilage are located between the condyle and fossa and serve as a cushion between the bone structures. The disk is attached to the maxilla with ligaments. During jaw movement, such as mouth opening,

chewing or speaking, the condyle rotates inside the articular fossa and slides along the articular eminence [3].

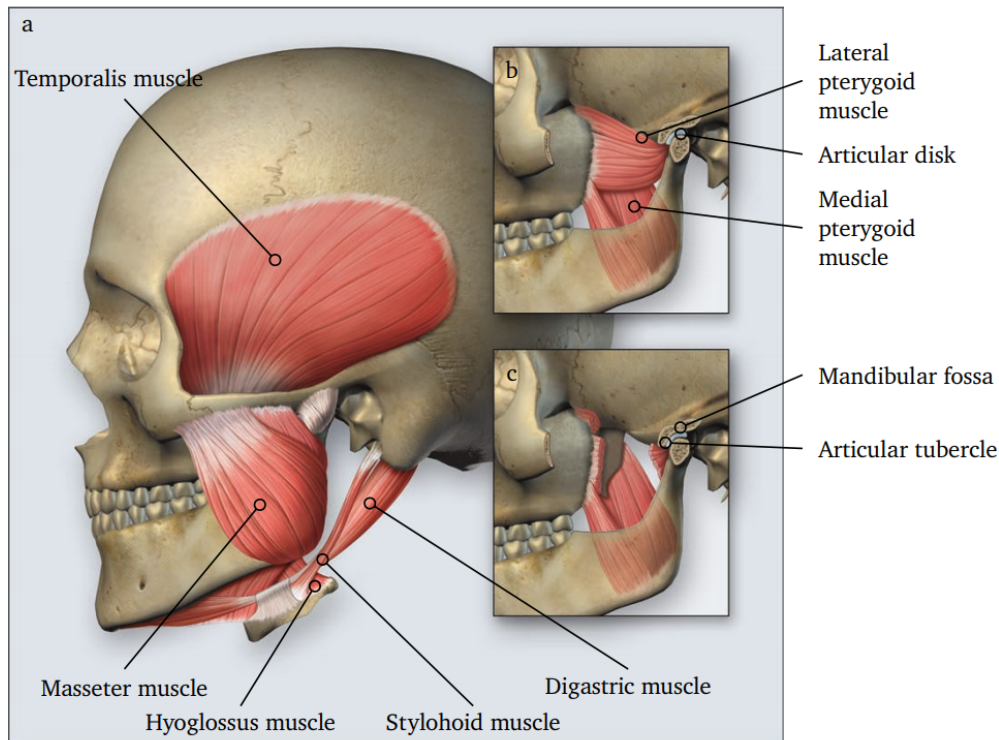


Figure 2.2.: Muscles associated with jaw function. [4]

The important muscles needed to perform jaw movement are depicted and labelled in Figure 2.2. The main mastication muscles are the temporalis and masseter muscles which are attached to the skull to lift and close the mandible. The other muscles involved in mastication are the medial and lateral pterygoid muscles which are located underneath the masseter (Panels B and C in the figure). Additionally, the anterior and posterior digastric and hyoid muscles beneath the chin are involved in any complex jaw movement. The jaw closing muscles, i.e. the temporalis, masseter and medial pterygoid muscles, are passively activated when the mouth is closed. During a jaw opening movement, these passive tensions have to be overcome to open the jaw. In comparison, the passive tensions of the jaw opening muscles are insignificant and so for jaw closing very little muscle activation is required [5]. With full muscle activation of the closing muscles, bite forces of up to 890 N can be reached in a healthy person [6]. Functional muscle groups for mouth opening, closing and lateral movements are summarised in Table 2.1. For mastication, a combination of all three movements is performed, involving all three muscle groups.

Any impairment concerning the TMJ, the masticatory muscles and associated head and neck musculoskeletal structures is termed a temporomandibular disorder [1] and can manifest itself in a restricted mouth opening range, deviation of the jaw during movement or a limited chewing function.

movement	involved muscles
mouth opening	anterior digastric, mylohyoid, lateral pterygoid
mouth closing	temporalis, masseter, medial pterygoid
laterotrusion	right or left inferior pterygoid

Table 2.1.: Functional muscle groups for mouth opening, closing and laterotrusion [7].

2.2. Kinematics of the mandible

Three different movement types for the mandible can be distinguished and described in separate planes: up-down motion in the frontal plane, side to side motions in the transverse plane and towards-backwards motion in the sagittal plane [8]. Mandibular motion is defined by the movement of the condyles. During mouth opening, the condyles first rotate for about 10° around the hinge axis, also termed condylar axis, going through the centre of both of the condyles, see Figure 2.3. Then, during further opening, a combination of rotating and translating forward along the temporal surface is performed. The centre of the condyle hereby follows a condylar path. For lateral movements, during chewing, for example, one condyle slides forward along the condylar path while the other stays fixed at any point on the path, thus resulting in the deviation of the jaw to one side.

Since the mandible is a rigid bone structure, all mandibular motion can be described by tracing a point at the lower incisors, the so-called incisal point (IP). The area that can be reached by this point is described by the Posselt Figure 2.3. It was first established in 1952 by Posselt [9]. The outline of this area is the border movement of the incisal point. Segment CR-B represents the initial mouth opening where the mandible only rotates. Afterwards, simultaneous translation and rotation of the mandible occur, forming segment B-E. Segment E-F describes the mouth closing movement with the condyles at maximum protrusion and segment CO-F is determined by the structure of the teeth.

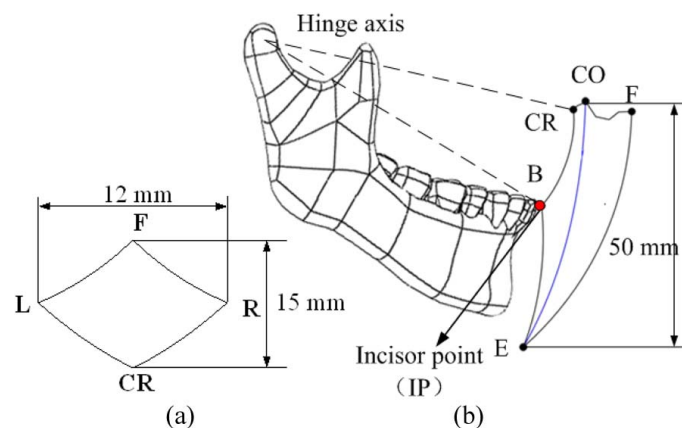


Figure 2.3.: Posselt figure: Maximal envelope that the lower IP can reach in (a) transverse plane and (b) sagittal plane [10].

3. Related Work

This chapter gives an overview of existing jaw rehabilitation devices used for the treatment of TMD and of existing attempts and approaches to biomechanically model the jaw.

3.1. Jaw rehabilitation devices

Currently, a range of devices of varying complexity is available to guide jaw movement. They are designed to rehabilitate the jaw after loss of muscle function or limited range of motion. The latter is often the case for patients suffering from TMD, therefore these devices are used for jaw rehabilitation, as well as the treatment of TMD, as they are often the same.

3.1.1. Insertion based devices

The simplest way to increase mouth opening distance is by inserting an appliance between the teeth to gradually increase the mouth opening. One method to do this is to put wooden spatulas between the teeth and keep stacking more spatulas to further open the mouth [11] (Figure 3.1a). This can also be done using a screw [12] (Figure 3.1b) and gradually turning it to increase mouth opening distance, or the Heister Jaw Opener [13] (Figure 3.1c) which has two tips that move apart when turning the handle of the device. Moreover, there is the TheraBite device [14] (Figure 3.1d), the most known commercially available device for increasing mouth opening range. It has two mouthpieces that move apart according to the force that is exerted by pressing the levers of the device.

All of these devices can be actuated by the patient themselves, thus the patient controls how far their mouth is opened and how much force is applied. Even though these methods are widely used by therapists and do speed up the rehabilitation process, they have to be repeated many times, the applied motion will neither be smooth nor repeatable, and it only allows rehabilitation in one plane, which limits the effectiveness of the treatments.



(a) Wooden Spatulas



(b) Screw



(c) Heister Jaw Opener



(d) TheraBite device

Figure 3.1.: Insertion based rehabilitation devices [8]

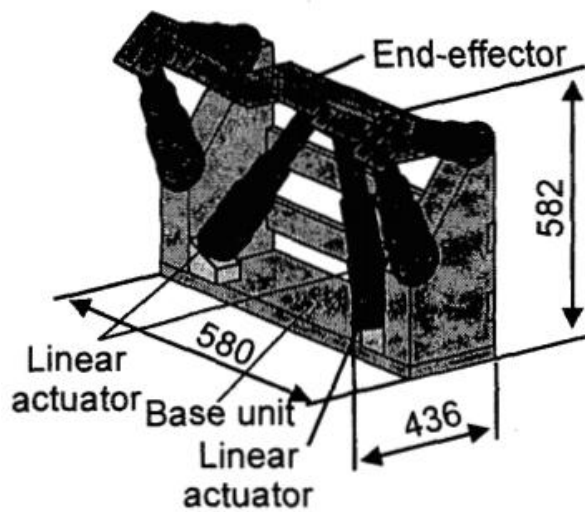
3.1.2. 6-DOF Parallel Robot

While also designed for mouth opening and closing training, the parallel robot WY-5 [15] is more advanced since it has actuators, sensors and a control system. It has six degrees of freedom (DOF) because even though normal jaw motion can be described by three or four DOF, motions of a dysfunctional jaw often need more DOF. The robot implements a master-slave system: One part is the 6-DOF patient manipulator with a u-shaped effector which is inserted into the patient's mouth and controlled by six linear actuators. The other part is the doctor manipulator which controls the patient manipulator and has only 2-DOF to perform an open-close and forwards-backwards movement. The patient manipulator continuously sends back force information so that bite force values can be controlled when actuating the doctor manipulator.

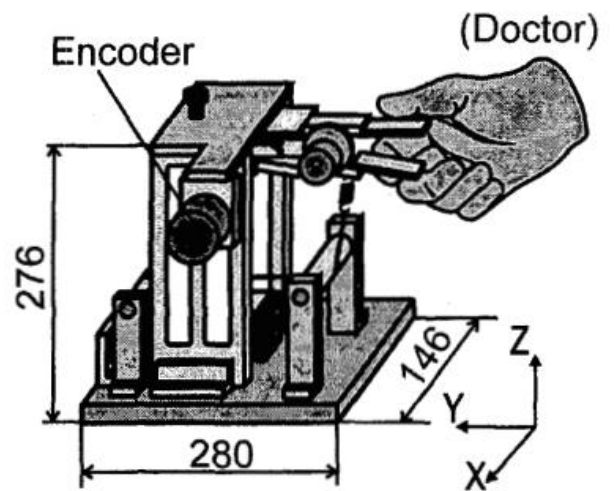
The parallel robot enables jaw rehabilitation in more than one plane, but again, the actuation is manual and therefore smooth and repeatable motion is not possible, limiting treatment effectiveness. Furthermore, treatment with the parallel robot requires the presence of a person operating the doctor manipulator. This in itself is an obstacle because of the limited availability of therapists.

3.1.3. A Novel Automated Device

Recently developed in 2020 by Koter and Pawe, the device presented in [8] provides rehabilitation in every degree of freedom. It consists of a movable frame and a pneumatic repulsion system. The



(a) Patient manipulator



(b) Doctor manipulator

Figure 3.2.: 6-DOF Parallel Robot WY-5 [15]

frame has two parts that can move independently in all three planes, controlled by pneumatic actuators. Attached to the frame is a mouthpiece for the upper and lower teeth and in between these mouthpieces, pneumatic bellows are placed. Testing of the effectiveness of this device regarding jaw rehabilitation treatment is still in the early stages.



Figure 3.3.: A Novel Automated Device [8]

3.1.4. Exoskeleton

A different type of device for jaw rehabilitation is the Shoulder-Mounted Robotic Exoskeleton [16]. It has a motor at each temporomandibular joint, rotating a mouthpiece around the condylar axis. The mouthpiece itself is not controlled but moves passively in the sagittal plane. Thus the exoskeleton allows motion in 2-DOF. The system also controls the amount of applied force and, in theory, therapy routines can be performed with the exoskeleton, although none have been implemented.

The EMG exoskeleton [17] works similarly and additionally has sensors that measure brain and muscle signals to detect jaw movement. Based on these signals, the desired rotational force of the motors can be calculated.



(a) Shoulder-Mounted Robotic Exoskeleton [16]

(b) The EMG Exoskeleton [17]

Figure 3.4.: Exoskeletons

The advantage of these exoskeletons is that they can be mounted on the shoulder and be worn daily. They provide programmable assisted therapy functions which help engage the user in the rehabilitation process and are therefore also helpful in the neurological rehabilitation of TMD. However, till now, these solutions are mere concepts and are still very limited. The control system is complex and, while therapy routines have been proposed, none have been implemented. Like most rehabilitation devices, they only allow 2-DOF movement.

3.2. Biomechanic modelling of the jaw

Early computational models of the jaw were static, two-dimensional rigid body models. One of the first dynamic, three-dimensional models was developed by Koolstra and van Eijden, 1997 [18]. Maxilla and mandible were modelled as rigid bodies and a flat occlusal surface was used for modelling tooth contact. The TMJ was simplified as frictionless contact between a spline surface and a sphere, representing contact between articular fossa and condyle as an interpenetration of the geometrical shapes. A muscle model was also included, relating muscle force to muscle activation, length, and velocity. Another approach was developed by Peck, Langenbach and Hannam, 2000 [19] who used an ellipsoidal condyle and a combination of multiple linear plates as the condylar path. Contact between the condyle and articular fossa and between the teeth were modelled the same as in the previously described model. The model by Stavness et al., 2006, (see Figure 3.5) is an adaptation of the Peck model in Open Source [7], using point constraints for the condyle to define mandible movement. Muscles were represented as Hill-type point-to-point muscles [20] and their velocity-force and length-force behaviour and cross-section area were defined with the help of previous literature [19], [21]. The model was developed using the Artisynt Modelling Toolkit [22] and for constructing the model geometry, they used high-resolution CT data of one male subject with normal jaw and TMJ function.

These models do not include a detailed temporomandibular joint, but since they accurately model the dynamic aspects of the jaw, they are valuable for the analysis of complex jaw movements and corresponding muscle activation patterns.

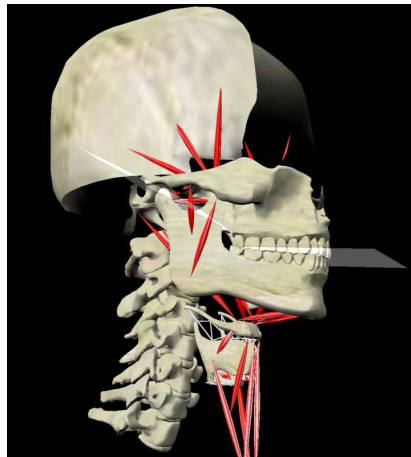


Figure 3.5.: Stavness et al., 2006 [7]

For example, Hannam et al., 2008, used the rigid body model from Stavness et al. for investigating open-closing motion and mastication [21]. It has also been used by Ackland et al., 2017, for evaluating the effect of joint replacement surgery on jaw function and joint loading [23].

Models that include detailed meshes of TMJ structures as Finite Element Models (FEM) have also been developed and are mainly used for analysing joint loading. However, they are often focused on modelling the TMJ only, neglecting muscle forces or dentition, and dynamic simulations of these models have a high computational cost.

The first model to combine a rigid body model of the jaw with finite element modelling of the joint was [24] by Koolstra and van Eijden in 2005 (Figure 3.6). They created a dynamic musculoskeletal model of the masticatory system with a FE model of the TMJ.

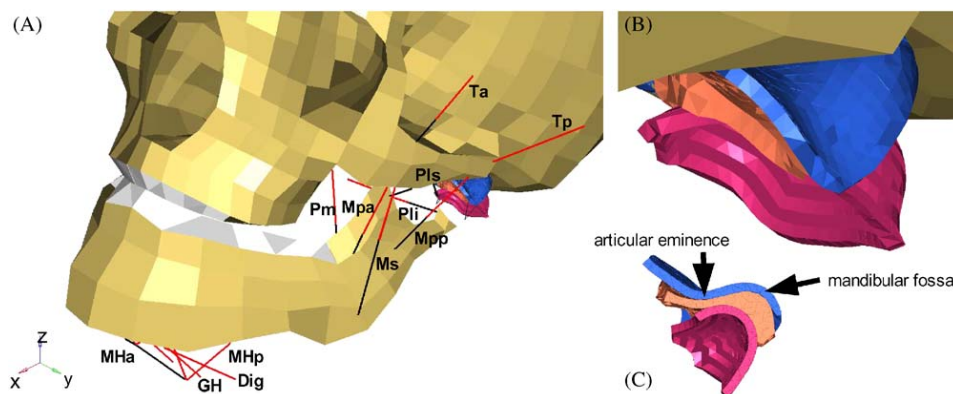


Figure 3.6.: Koolstra and van Eijden, 2005 [24]

Based on this, Sagl et. al only recently (2019) [25] incorporated a detailed finite element model (FEM) disk and an elastic foundation (EF) articular cartilage into the rigid body model by Stavness et al. [22], enabling a detailed analysis of von Mises stresses and stress distribution in the joints with much shorter simulation times than the outdated model from Koolstra and van Eijden.

These are the most widely known models, however, further models exist ([26], [27]). They differ in whether they are dynamic, or muscle-driven, or use point constraints for the condyle, and especially in how the TMJ is modelled. This can include a FEM Disk (Sagl), Articular Cartilage, FEM Ligaments, or none of these. Additionally, many models do not use individually modelled joints but only model one joint and then mirror it.

To summarise, several biomechanical models of the jaw exist and have been used to analyse chewing, jaw opening, muscle activation, and joint loading during movement.

However, they have each been modelled according to the anatomy of one person and depict perfectly normal jaw function. To the best of the author's knowledge, these models have not been used to simulate any dysfunctions in the jaw yet, which could be important for the development of effective treatment strategies for such dysfunctions. The need arises for a model which can be personalised to a patient and appropriately models any dysfunction in the jaw so that the dynamics of a dysfunctional jaw can also be analysed and treatment strategies investigated. Therapy routines can then be adapted to the patient's individual needs with previous simulation and evaluation by software, allowing a new, personalised TMD treatment.

3.3. Kinematic modelling of mandibular movement

3.3.1. Revolute joints

An early kinematic model for jaw movement was proposed by Weingärtner, Haßfeld and Dillman in 1997 [28]. Their model relates the motion of the jaw to rotations in the joint. It “consists of a sequential open-loop chain with rigid bodies connected by revolute joints”. They identified three movements, the combination of which can describe any possible position of the incisal point. These movements are the opening movement around the hinge axis, the protrusion of the condyles, and the lateral movement. Each movement is modelled as a simple rotation for which the rotation axis has to be determined.

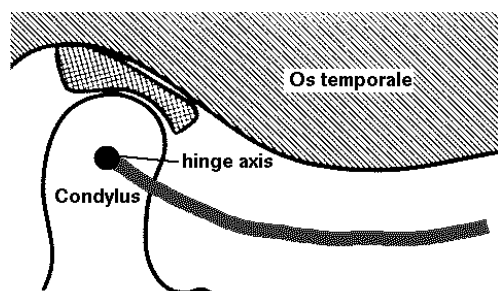
The rotation axes are depicted in Figure 3.7b. The axis for the opening movement is simply the hinge axis R_h . For protrusion of the condyles, the condylar path was modelled as a section of a circle. The rotation axis R_p was the circle centre, located somewhere on the Os temporale (see Figure 3.7a). The exact position of this point depends on the individual patient anatomy. Lastly, the rotation axis for lateral movement R_{lp} depends on the movement side. In a left lateral movement, the left condyle stays in place while the right condyle is protruding. The rotation axis, therefore, goes through the left condyle and the rotation point of the protrusion of the right condyle. Right lateral movement can be described analogously.

The coordinates and orientation of the incisal point are then given by the following equation, which represents the forward kinematics model:

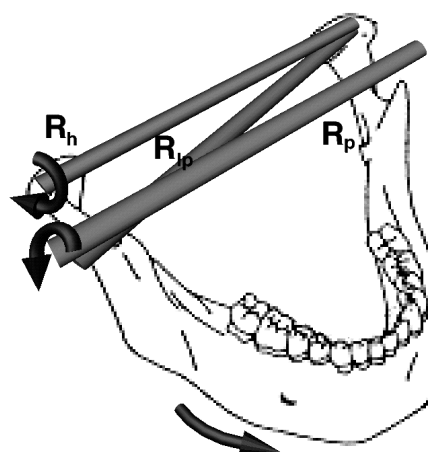
$$I(\Theta_p, \Theta_{lp}, \Theta_h) = F_0 \cdot R_p \cdot T_1 \cdot R_{lp} \cdot R_h \cdot T_2,$$

with Θ_p , Θ_{lp} and Θ_h describing the rotation angles around the corresponding axes. All transformations are homogeneous, and the translations F_0 and T_i are defined by individual patient anatomy.

As a solution for the inverse kinematic problem, the authors proposed a machine learning and a gradient descent approach. With this method, the rotation angles for all incisor points in the Posselt envelope of a test person could be determined. However, the model is a simplification of mandibular kinematics and does not accurately describe all movements of the mandible. The condylar slope varies from patient to patient and in most cases, cannot be accurately modelled as the segment of a circle. Additionally, with only three degrees of freedom, only limited movement patterns can be reproduced. Especially for modelling the kinematics of a jaw with indications for TMD, where motion is often asymmetrical, more degrees of freedom and a combination of rotation and translation of the condyle is necessary.



(a) Condylar path as segment of a circle



(b) Kinematic axes for left side movement

Figure 3.7.: A kinematic model with three revolute joints. [28]

3.3.2. Non-orthogonal floating axis joint coordinate system

Leader et al. developed another model for describing mandibular motion, using a non-orthogonal floating axis joint coordinate system with 6-DOF [29]. For defining this system, Cartesian coordinate frames were defined for maxilla and mandible. Initially, these are in the same position, with the midpoint of the condylar hinge axis being the origin of both frames. A third frame describes the relation of the mandible to the skull during movement or at rest. This frame connects the maxilla and mandible coordinate systems and is therefore a joint coordinate system with a floating axis. Figure 3.8 shows the orientation of all three coordinate systems and how the coordinate axes are defined. The first axis of the joint coordinate system e_1 represents the x-axis of the maxilla, and e_3 represents the z-axis of the mandible. The floating axis e_2 is perpendicular to e_1 and e_3 and intersects both axes. The rotation around e_1 , e_2 and e_3 is described by α , β and γ . A rotation around e_1 causes a mouth opening motion, rotation around e_2 corresponds to the condyles moving inferiorly

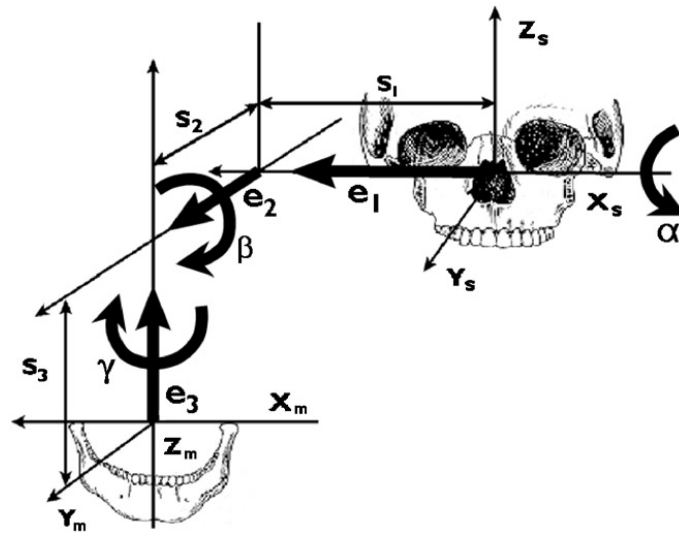


Figure 3.8.: Orientation of the non-orthogonal floating axis joint coordinate system. [29]

or superiorly and finally rotation around e_3 corresponds to the posterior-anterior movement of the condyles. Translation along these axes are defined by S_1 , S_2 and S_3 .

The joint coordinate system is treated as a system of six 1-DOF joints that are either revolute or prismatic. For calculating rotation angles and translation distances, inverse trigonometric functions and substitution were used.

With 6-DOF, mandibular motion can be fully described. However, the model was only used for mouth opening movements in healthy patients, with translation only in the sagittal plane. The authors analysed correlations of the parameters S_2 , S_3 and α (which describe the transformation in the sagittal plane) during the mouth opening movement, with all other parameters close to zero. No further analyses were conducted on the value of the other parameters S_1 , β and γ during other movement patterns.

While this model allows capturing the full range of movement of the mandible, there are no constraints on the movement of the condyles. For a more accurate kinematic model, limitations on condylar movement have to be considered as well.

3.3.3. Higher kinematic pair TMJ

Wen et. al defined a kinematic model describing mandibular motion for the development of a jaw movement robot [10]. They modelled the TMJ as a higher pair kinematic joint. The kinematic axis of this pair was the condylar hinge axis, i.e. the line passing through the condyle centre points. The displacement of the condyles was given by a two-dimensional surface:

$$Z = 0.0052X^3 - 0.072X^2 - 0.3837X \quad (3.1)$$

This is the condylar surface, shown in Figure 3.9 as two slopes S_1 and S_2 . The red circles in the figure represent the condyles in their initial position and the blue circles during movement.

The position of the mandible is described by an instantaneous reference frame O_I which initially, at teeth occlusion, coincides with the mandible frame O_M . The origin of both is located at the midpoint of the kinematic axis. At every moment, mandible movement has 4-DOF. An instantaneous plane P can be determined which includes the kinematic axis and is otherwise defined by the articular slopes, see Figure 3.9. The 4-DOF are then as follows: rotation β_{RI} around the kinematic axis, rotation δ_{RI} around an axis which is a normal vector to the instantaneous plane P and goes through O_I , and translations Y_{TI} and W_{TI} along the two dimensions of the plane P .

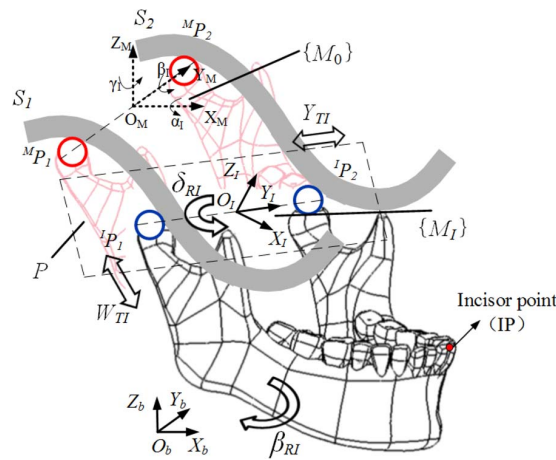


Figure 3.9.: 4-DOF mandibular motion [10]

The position and orientation of the instantaneous frame can be described as a 6-DOF transformation of the fixed mandible frame. Since this then has 6-DOF but the actual movement has only 4-DOF, the angles α_I and γ_I and translations X_I and Z_I are correlated. Therefore only four parameters have to be specified to describe the transformation as the other two can be derived from these four parameters.

3.3.4. Instantaneous centre of rotation

In the previous models, the hinge axis passing through the condyle centres was assumed to be the rotation axis for mandibular movement. However, studies have shown that there is no fixed centre of rotation during mandibular movement [30]. Instead, an instantaneous centre of rotation (ICR) is assumed. This means that at any given moment, a rotation axis around which the mandible rotates can be determined and this axis differs greatly from the traditional hinge axis.

Figure 3.10 shows the movement of the instantaneous centre of rotation during the opening and closing movement as computed by Ahn et al. [30]. At the beginning of the opening and end of the closing movement, the ICR is, despite moving, relatively close to the hinge axis. But with increasing inter-incisal distance, the ICR moves further away from the condyle centre.

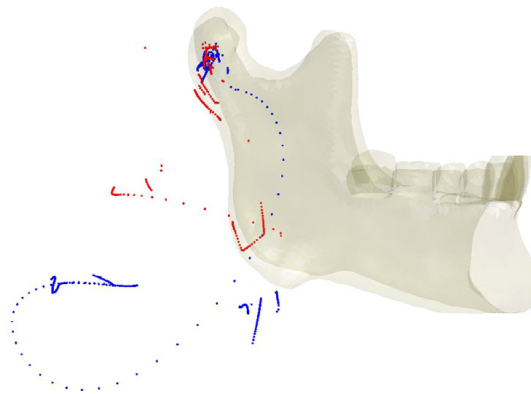


Figure 3.10.: ICRs during opening movement is represented by blue points, while red points show ICRs during closing. [30]

While this points out inaccuracies using the hinge axis as the rotation axis, calculation of the ICR is more complex and has to be done every step of a simulation. Moreover, there are various methods to calculate the ICR and calculated ICR locations are very inconsistent across the different methods [30].

3.4. Conclusion

To conclude, multiple devices for the treatment of TMD are already available. Each provides different treatment options, making TMD therapy very diverse in technique and application. By offering a device that allows repeatable therapy for a variety of symptoms, therapy could be standardised and treatment of the existing devices integrated into one device. An active, intelligent orthosis, as proposed in this research, combines the advantages of existing devices and offers more flexibility in treatment options. Therapy can be adapted to suit a wide range of TMD symptoms and causes and it can be personalised to the patient in terms of the range of motion and difficulty level. The orthosis enables jaw rehabilitation in all movement directions and helps with neurological rehabilitation. Furthermore, such an orthosis can track the progress of a patient over time and help with characterising TMD by providing a standardised measure of patient performance.

The development of such a device requires a kinematic model describing its range of motion, which corresponds to that of the mandible. Such models already exist and will be adapted and integrated into the orthosis system. For the development and evaluation of the orthosis, a biomechanical model of the jaw is needed. Existing jaw models are created from the anatomy of one, healthy person, which limits their use for the development of personalised therapy. Before the orthosis can be used on an actual patient, the system has to be tested on a patient-specific model. Since it is not feasible to create a new, biomechanical model for every patient who seeks TMD treatment, a generic jaw model, which can be personalised to the patient, is needed. An existing jaw model will be adapted to factor in personalisations and TMD symptoms. Based on this model, trajectory following and

resistance training therapy routines, which have been suggested for the exoskeletons [16], will be implemented.

4. Jaw Modelling

This chapter introduces the biomechanical model used for the simulation of the jaw and the temporomandibular joint. The model was extended with the articular disk (Section 4.2.1) and adapted to factor in patient-specific anatomy (Section 4.2.2) or TMD signs (Section 4.3), so that it can be personalised to the patient. The jaw model with TMD symptoms is used in Chapter 6 for the evaluation of developed therapy routines.

4.1. The biomechanical model

For modelling and simulating the temporomandibular joint and the jaw, the ArtiSynth Toolkit [7] is used. With ArtiSynth, biomechanical models can be built using a combination of multibody and finite element models (FEM). The software already includes a dynamic rigid body model of the jaw and laryngeal structures. A big advantage over other existing jaw models is that the software is Open Source. The system is implemented in Java.

For the biomechanical jaw model in ArtiSynth, model geometry was created using CT images of a 35-year-old, asymptomatic person. Muscle properties and other parameters in the model were taken from established literature. Muscles are of Hill-type [20] and bite contact and TMJ displacement is constrained by Lagrangian rigid-body constraints.

Jaw movement is caused by the excitation of the muscles, and can also be manipulated by applying external forces on the jaw. Muscle activation for a simulation is programmable, or it can be passed as an input probe to the simulation. It is also possible to activate the muscles manually during the simulation. ArtiSynth already includes an input probe containing the muscle activation levels for a chewing movement. This probe was used for simulating chewing, whereas mouth opening-closing was simulated by steadily increasing muscle activation of the opening muscles, given in Table 2.1, and then steadily decreasing it again. Laterotrusion was simulated similarly, with activation and deactivation of the right or left inferior pterygoid muscle. Additionally, the mouth opening muscles were activated a little, to increase the stability of the lateral movement, as was done by Sagl [25].

While an output probe of the simulation existed for the trace of the lower incisor, probes were added for the mouth opening distance and angle, see A.3. The opening distance was measured as inter-incisal distance. The opening angle was calculated as the angle between upper and lower incisors in the sagittal plane, about the midpoint of the condylar axis. These measures are often

used for the classification of TMD and assessment of temporomandibular joint mobility [31]. In jaw rehabilitation, mouth opening distance is measured as a way to track treatment success.

The ArtiSynth Toolkit includes a Jython interface, for manipulating the simulation and handling simulation results in python. The Jython console was used for repeatedly starting a simulation with different parameters, especially for the evaluation of the therapy routines, and for automatically exporting output probes, which otherwise would have to be done manually in the GUI. Implemented Jython scripts are appended (A.2) and detailed instructions on how to run and modify simulations are given in the documentation, see <https://github.com/laura-jehn/jaw-modelling-thesis>.

4.2. Personalising the model

4.2.1. Articular disk

Many TMDs are related to the articular disk. It is common in TMD that disk displacement occurs. This means that the disk is dislocated anteromedially to the condyle. There are two forms of disk displacement: with or without reduction. In disk displacement with reduction, the dislocation only occurs when the condyles are almost fully protruded, whereas without reduction, the dislocation is permanent. This can severely affect the range of motion of the jaw and joint loads in the TMJ. Therefore, having a model with the articular disk is essential for modelling TMD.

The disk has previously been modelled by Koolstra and van Eijden [24] and by Sagl [25], although their implementations are not publicly available. They created a model of the disk from MRI data which is very intricate and requires a lot of work. A simpler model can be created from the surface of the condyles since the disk is deformable and adapts to the shape of the condyle and articular fossa.

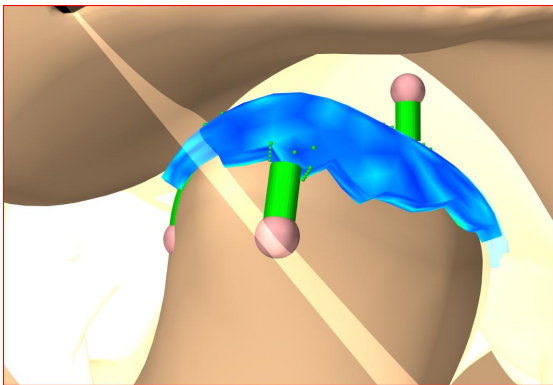
For this, the surface mesh of the jaw was exported to MeshLab and vertices and faces deleted so that only a mesh of the condylar surface remained, see Figure 4.1b. The faces of the mesh were triangular and some of them were very long and thin. This can lead to problems with numerical stability in the simulation. Therefore the mesh was reconditioned using an Isotropic Explicit Remeshing filter in MeshLab with a desired triangle edge length of 0.5mm. As a result, the mesh had 383 vertices, 700 faces and all triangles were equilateral.

A finite element model (FEM) of the disk was created by extruding the condylar surface mesh along the normal direction of its faces. A hyperelastic Mooney-Rivlin material was used for the FEM, the strain energy density function of which is defined by two constants $C1$ and $C2$. For the articular disk, the constants were $C1 = 9 \cdot 10^5 Pa$ and $C2 = 2 \cdot 10^5 Pa$, taken from [25].

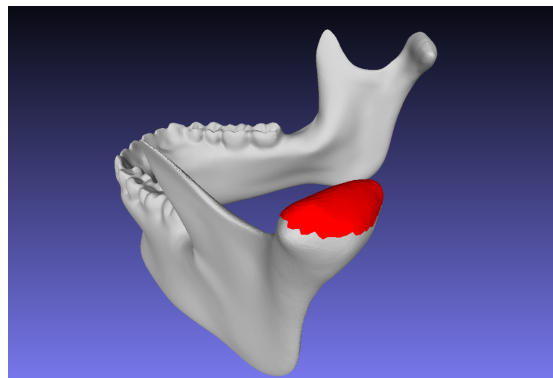
The disk is held in place by the articular cartilage and surrounding structures. This was modelled by attaching the FEM to the condyle and the maxilla with ligaments, as was done in [25]. The ligaments are each attached to ~ 20 nodes of the FEM to distribute the exerted force over several elements.

The resulting FEM had 2800 wedge elements and is visualised in Figure 4.1a. The larger the number of elements in the FEM, the better the calculation of disk shape and stress. But with an increasing number of elements, the computational cost also increases. The number of elements was therefore chosen so that simulation time was still reasonable. On an I7-4790k processor, a simulation of one second took three minutes. In a future model, the number of elements can be increased for more accuracy.

For increasing numerical stability, the maximum step size of the simulation was set to 0.001 seconds and a Constrained Backward Euler integrator, available in ArtiSynth, was used.



(a) Screenshot of the disk in ArtiSynth.



(b) Surface mesh of the jaw and the condyle surface in MeshLab.

Figure 4.1.: Creation of a FEM of the articular disk.

A small mouth opening movement can be performed with the disk, however, some difficulties remain concerning its dynamic properties, specifically numerical instability is a problem.

The encountered difficulties are further described in the appendix (A.4.2) and the Java class for creating the disk is also appended (A.4.1).

4.2.2. Condylar slope

The condylar slope differs from patient to patient. It is relevant for personalised orthosis development since it has a big impact on the incisor trajectory.

Coutant et. al [32] identified three groups with different average condylar slope inclinations. For each group, they determined the rotatory and translatory components during mouth opening. At the beginning of the opening phase, both translation and rotation occur. Depending on the group, with a greater mouth opening distance, the rotatory component may become more prominent. On the one hand, there is the rotatory preponderant group (RG) where maximum mouth opening is associated with a considerable rotatory component. At the end of the mouth opening movement, an almost pure rotation occurs. The average slope inclination for this group is 47.25° . On the other hand, there is the translatory preponderant group (TG) where even during maximum mouth opening, the ratio of rotation and translation stays the same, with an average slope inclination of 18.28° . In the middle

group (CG), the rotatory component is more prominent but less than in the RG. For this group, the average slope inclination is 30.42° . Displacement values along the sagittal axis for the condyle centre during maximum mouth opening are also given for two zones on the temporal surface. The first zone is the articular tubercle slope (ATS), or articular eminence, which corresponds to the first part of the condylar slope and is more or less linear. Then, the condyle passes the articular tubercle crest (ATC), where the ATS is curved. Finally, the condyle reaches the preglenoid plane (PP), the part of the temporal surface after the ATC. Displacement values for ATS and PP are: 6.12mm / 3.75mm for RG, 11.42mm / 9.5mm for TG and 10.52mm / 4.52mm for CG. The different zones are illustrated in Figure 4.2, where α , x_{ATS} and x_{PP} correspond to the inclination and displacement values given for each group.

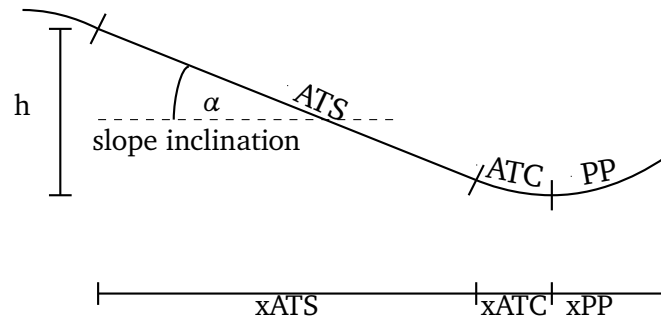


Figure 4.2.: Illustration of the parameters defining the condylar slope.

From these values, three distinct condylar slopes were approximated. According to Coutant et al [32] the condylar slope is described by a linear portion, followed by a non-linear portion. For approximating the curve, they used a cubic polynomial, cf. Equation 3.1. Here, in a similar approach, a parabola was used to approximate the part of the condylar slope before the ATS, which coincides with the articular fossa, then a linear approximation of the ATS follows and finally, the ATC and PP are again approximated by a parabola. Equation 4.1 describes the approximation for the ATS, ATC and PP zone. Using the given values α , x_{ATS} and x_{PP} for the approximation, one degree of freedom remained and, therefore, x_{ATC} was chosen to be 2mm.

$$condylar_slope(x) = \begin{cases} \tan(\alpha) \cdot x & \text{if } x < x_{ATS}, \\ -\frac{\tan(\alpha)}{2 \cdot x_{ATS}} \cdot (x - x_{ATX})^2 - h & \text{if } x < x_{ATX} + x_{PP}, \end{cases} \quad x \in [0, x_{ATX} + x_{PP}] \quad (4.1)$$

where $x_{ATX} = x_{ATS} + x_{ATC}$ and x_{ATS} , x_{ATC} , x_{PP} , h and α are defined in Figure 4.2.

The approximated slopes are visualised in Figure 4.3, where X describes the forwards-backwards movement of the condyle and Z describes the upward-downward movement. The maximum X displacement of 15 mm and Z displacement of 7 mm are consistent with reported maximum displacement values of the condyles during mouth opening [29].

For a comparison of the jaw movement with different condylar slopes, the approximated slopes were used as constraints for the condyles of the jaw model. In ArtiSynth, the constraint for each condyle

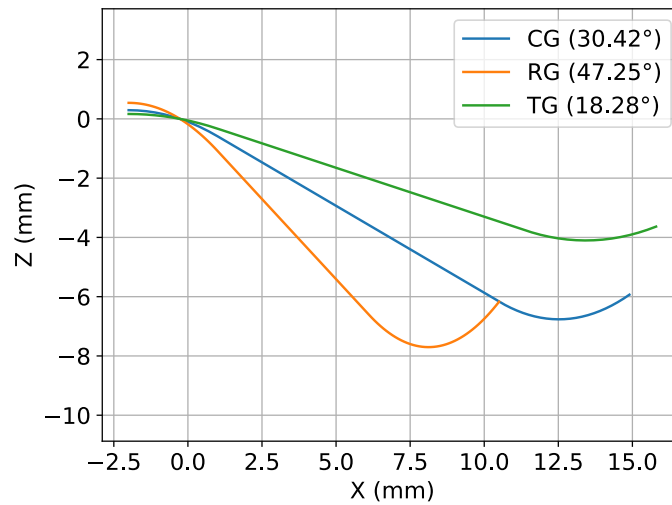


Figure 4.3.: Approximation of the condylar slope for different slope characteristics.

is defined by a point array which is internally converted to a two-dimensional surface on which the condyle can move. Point arrays were generated for the approximated slopes and added to the jaw model (`JawModel.java`), and a variable was introduced for switching between the different types of the condylar slope.

```
public enum CondylarSlopeType {RG, CG, TG};
// default slope is CG, since this slope type is the most prevalent
static CondylarSlopeType condylarSlopeType = CondylarSlopeType.CG;
```

For each of the slopes, a mouth opening-closing movement was performed by activating and deactivating the mouth opening muscles, and the resulting incisor trajectories were plotted in Figure 4.4. The movement begins at teeth occlusion and ends in a resting position where the mouth remains slightly open because no muscles are activated. The figure shows that the condylar slope has a huge influence on the incisor movement which is why the slope must be taken into account when developing personalised therapy routines. For example, if the patient is asked to follow a given trajectory with their jaw, the trajectory must fit the healthy movement of the patient. Otherwise, following the trajectory could cause more strain on the patient's muscles and TMJ, effectively being counterproductive to the therapy.

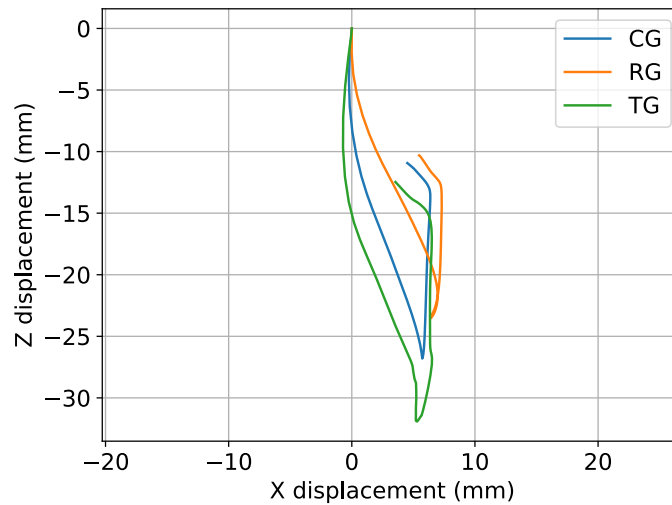


Figure 4.4.: IP trace during mouth opening-closing for the condylar slopes given in Figure 4.3, in the sagittal plane.

4.3. Modelling TMD

4.3.1. Limited range of motion

A limited range of motion of the jaw is a common symptom of TMD. The jaw movement can be limited in any direction, however, for the classification of TMD and its severity, mainly limited mouth opening range is considered. Inter-incisal distance is measured to quantify the maximum mouth opening range. A healthy range is between 35-55mm [8], if the maximum opening distance is less than 35mm, this implies that the patient suffers from TMD. A cause for restricted mouth opening range is often compromised muscle function. This can be either directly related to muscle problems or due to pain while moving the muscles which neurologically prevents the patient from fully using the muscles. Therefore, with a restricted mouth opening range the force exerted by the muscles will also be significantly lower.

In order to model this scenario of TMD, a patient's muscle function can be measured and the corresponding maximum muscle force can be set as a limit for the modelled muscles in the biomechanical model. If no patient data for muscle function is available, maximum muscle forces in the model can be approximated from the measured mouth opening distance.

To do this, the maximum muscle force of the opening muscles is reduced by a certain percentage. Due to a lack of data for individual muscles, the muscle force of all muscles involved in mouth opening is reduced equally. Mouth opening muscles are anterior digastric, anterior and posterior mylohyoid, inferior and superior lateral pterygoid and geniohyoid muscles (cf. Table 2.1). Mouth opening distance is measured at maximum muscle activation.

The following code excerpt from `JawModel.java` illustrates the reduction of the maximum muscle force exemplarily for the left inferior pterygoid muscle.

```
double ipMaxForce = 66.9; // Newton
double maxMuscleForcePercentage = 0.8;
// add lip muscle to model
// parameters: name, max force, optimal length, max length, tendon ratio
myMuscles.add(createPeckMuscle("lip", maxMuscleForcePercentage*ipMaxForce,
    31.5, 41.5, 0.0));
```

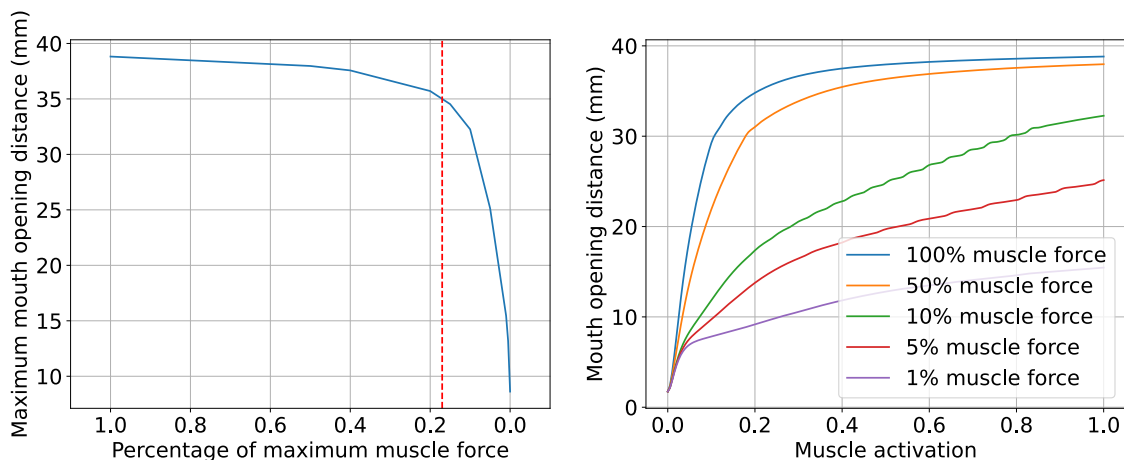


Figure 4.5.: Correlation between reduced maximum muscle force and maximum mouth opening distance and muscle activation and opening distance.

As Figure 4.5 shows, if the maximum muscle force of the opening muscles is reduced to up to 50%, this only has a small effect on the opening distance. This is because in a healthy jaw with large muscle forces, a small activation of the opening muscles is responsible for most of the mouth opening movement, see the right plot of Figure 4.5. Activating the muscles beyond 20% only has a small effect on further opening because at this point mouth opening is restrained by other factors like bones and ligaments and it is not anatomically possible to open the mouth any further. Therefore maximum muscle forces in the model need to be reduced to 17% or lower to significantly influence the opening range. For a reduction to 17% or less, the maximum opening distance is below 35mm, effectively modelling a jaw afflicted with TMD. When the opening muscles cannot be activated at all, i.e. the maximum muscle force is set to zero, the opening distance is still around 8mm because, at rest, the mouth is slightly open.

This is not an accurate model of the actual muscle function in patients with TMD. Nonetheless, it can be used to reproduce the range of motion of a patient in the model. This is valuable for developing orthosis and therapy routines, where mouth opening distance is important rather than the underlying causes. Muscle impairments can have multiple and complex causes, like injury or scarring of the muscles. Modelling these impairments in the scope of this model or even measuring them in a patient is not feasible.

4.3.2. Reduced bite force

Reduced bite force can be modelled similarly, by reducing the maximum force of the closing muscles: the anterior, medial and posterior temporalis, the masseter and the medial pterygoid muscles. The bite force is measured at the molar region since this is where food is crushed. Maximum bite force in this region is up to 890 N, whereas, at the incisors, maximum bite force is reported to be only 111 N [6]. In the simulation, the maximum reachable bite force at the molar region is 650 N. Maximum bite force and maximum muscle forces of the closing muscles are linearly correlated, as shown in Figure 4.6.

The bite force of the biomechanical jaw model can be measured by placing a food bolus between the teeth. The food bolus is modelled as a force effector with a certain resistance. When the bite force of the jaw is higher than the resistance of the food bolus, the bolus “collapses”, meaning that its resistance is set to zero. By setting the resistance of the food bolus very high, where it cannot be crushed, the maximum bite force of the jaw can be determined. Opening muscles are activated until a reasonable mouth opening is reached, i.e. the food bolus is between the teeth. Then, the closing muscles are fully activated. The resulting force at the food bolus is the maximum bite force of the jaw. Bite force can be evaluated at different mouth opening distances by adjusting the bolus diameter. For larger mouth opening distance, the maximum bite force decreases.

It follows that the maximum bite force of a patient can be measured, and can then be reproduced in the model by adjusting the maximum muscle forces of the closing muscles.

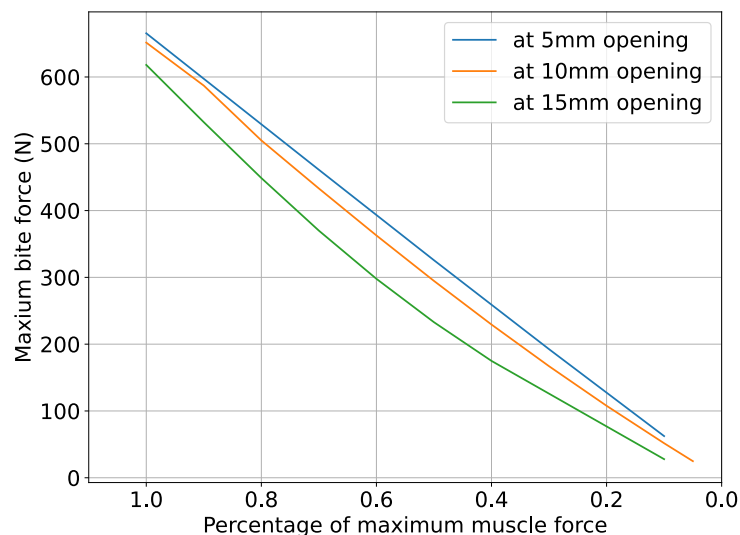


Figure 4.6.: Correlation between reduced maximum muscle forces and maximum bite force in the molar region at different opening distances.

4.4. Conclusion

With the presented methods, the ArtiSynth jaw model can be personalised to the patient in a few key aspects. One of these aspects is the condylar slope, which determines the movement of the mandible. Slopes were approximated for three common groups with different characteristics of the condylar movement. This allows some personalisation, but also requires the determination of the group to which the patient belongs.

Furthermore, common cases of TMD were addressed, making it possible to use the model for the development of therapy routines specifically targeting the modelled TMD symptoms. These include a limited mouth opening distance and a limited bite force, which can be modelled by reducing the maximum muscle forces of the corresponding muscle groups. While a simple model of the articular disk was integrated into the jaw model, disk-related TMD factors have not been modelled yet.

Anything related to the structure of the bone and teeth could not be personalised because this requires patient-specific MRI data. In particular, this concerns malocclusion, i.e. the misalignment of the teeth, which is strongly correlated to TMD [33]. In order to address such TMD cases in the model, MRI data could be acquired for typical occlusal schemes, such as an overbite or an underbite. From the MRI data, meshes could be generated, and depending on the occlusion type of the patient, the corresponding mesh could be used for the jaw model.

For the personalisation of the model, measurements have to be performed on a patient. Recently, Suppelt [4] developed a device for the measurement of TMD symptoms and the resulting jaw motion. This device allows measuring the mouth opening distance and the bite force of a patient and could help with including further TMD symptoms in the model, such as an asymmetrical jaw motion.

The jaw model can be evaluated in a dynamic simulation, requiring the muscle activations for producing a certain jaw movement, and, optionally, any external forces acting on the jaw. The simulation outputs the IP trace, the mouth opening distance and angle, and the bite force if there is a bolus resistance between the teeth.

5. Orthosis Development

In this chapter, the basis for the development of an orthosis is worked out. In this context, a kinematic model for describing the reachable area of the orthosis is presented and possible therapy routines are developed. The orthosis framework and its application for the realisation of therapy routines are evaluated in Chapter 6.

5.1. Kinematic model

As described in Section 2.2, the mandibular movement mainly consists of condylar rotation around the hinge axis and condylar translation along the temporal surface. Small translations and rotations in other directions can also occur, especially when the jaw is compromised by TMD. For this reason, each joint has three rotational and three translational DOFs but the movement is constricted by bone collisions and joint ligaments [10]. Because the joints are connected by the jaw, modelled as a rigid body, a kinematic model for mandibular movement simultaneously describes the position and orientation of the condyles. The mandible has then potentially 6-DOF, but with constraints on the displacement of the condyles. According to Okino [34], the 4-DOF shown in Figure 5.1 are sufficient for describing mandibular movement. The 4-DOF include rotation around the kinematic axis, protrusion of each of the condyles and a very small lateral translation of the condyles. This lateral translation may be larger in dysfunctional jaws.

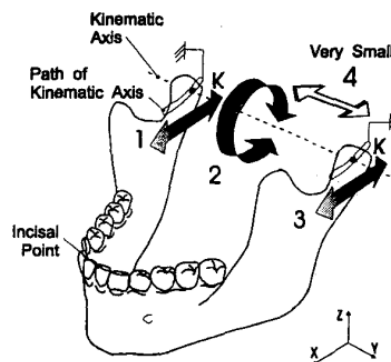


Figure 5.1.: Degrees of freedom of the mandible. [15]

It follows that a kinematic model describing the full movement range of the mandible must have 4-DOF with constraints for the displacement of the condyles and constraints on the reachable incisor position. All of this is already taken into consideration in the kinematic model as described by Wen [10] (see Section 3.3.3).

An orthosis for jaw rehabilitation should also have 4-DOF to reproduce full jaw motion. The kinematic model, therefore, corresponds to the range of movement of the orthosis.

The kinematic model was implemented in Python.

5.1.1. Forward kinematics

Mandible position at an instantaneous moment is described by the homogeneous transformation matrix [10]

$${}^M T_I = \begin{pmatrix} c\gamma \cdot c\beta & -s\gamma \cdot c\alpha + c\gamma \cdot s\beta \cdot s\alpha & s\gamma \cdot s\alpha + c\gamma \cdot s\beta \cdot c\alpha & X \\ s\gamma \cdot c\beta & c\gamma \cdot c\alpha + s\gamma \cdot s\beta \cdot s\alpha & -c\gamma \cdot s\alpha + s\gamma \cdot s\beta \cdot c\alpha & Y \\ -s\beta & c\beta \cdot s\alpha & c\beta \cdot c\alpha & Z \\ 0 & 0 & 0 & 1 \end{pmatrix}, \quad (5.1)$$

where c is cosine and s is sine. This matrix transforms a point from the instantaneous frame to the mandible frame. The mandible frame is fixed and has its origin at the midpoint of the condylar axis at teeth occlusion. The alignment of the axes is the same as in Figure 5.1. The instantaneous frame initially coincides with the mandible frame but is transformed by the translations X , Y and Z and rotation angles α , β and γ around the respective axes, see Figure 3.9.

The movement is constrained by the condylar slope in the sagittal plane, given by a continuously differentiable function, cf. Equation 4.1 and Equation 3.1, relating the X -translation of the condyle to its Z -translation. The slope should be patient-specific, as described in Section 4.2.2. Due to the slope, a correlation exists between the translations X and Z and the angles α and γ . Both condylar points P_1 (right) and P_2 (left), and the origin of the instantaneous frame O_I are determined:

$$\begin{aligned} {}^M P_1 &= {}^M T_I \cdot {}^I P_1 \\ {}^M P_2 &= {}^M T_I \cdot {}^I P_2 \\ {}^M O_I &= 0.5 \cdot ({}^M P_1 + {}^M P_2) \end{aligned}$$

The distance between the condylar points is constant. When X , Y , β and γ are given, α and Z can be determined with these equations, using a numerical solver for the following nonlinear equation system:

$$\begin{aligned} slope(x1) &= z1, \text{ where } x1, z1 \text{ are the } x, z \text{ components of } {}^M P_1, \\ slope(x2) &= z2, \text{ where } x2, z2 \text{ are the } x, z \text{ components of } {}^M P_2, \\ z_o &= Z, \text{ where } z_o \text{ is the } z \text{ component of } {}^M O_I \end{aligned}$$

As a result, we have six parameters with two constraints, leaving 4-DOF. Given the four parameters X , Y , β and γ at an instantaneous time, the position of the incisor point $IP \in R^{4 \times 1}$ can be calculated using the transformation matrix:

$${}^M IP = {}^M T_I(q) \cdot {}^I IP, \quad q = (X \ Y \ \beta \ \gamma)^T, \quad (5.2)$$

where ${}^M IP$ is the incisor point in the mandible coordinate frame and ${}^I IP$ is the incisor point in homogeneous body coordinates. ${}^I IP$ is fixed because the IP moves with the instantaneous frame. For the ArtiSynth jaw model, the body coordinates of the lower incisal point are given below.

$${}^I IP = (79.41 \ 0 \ -37.87 \ 1)^T$$

5.1.2. Parameter boundaries

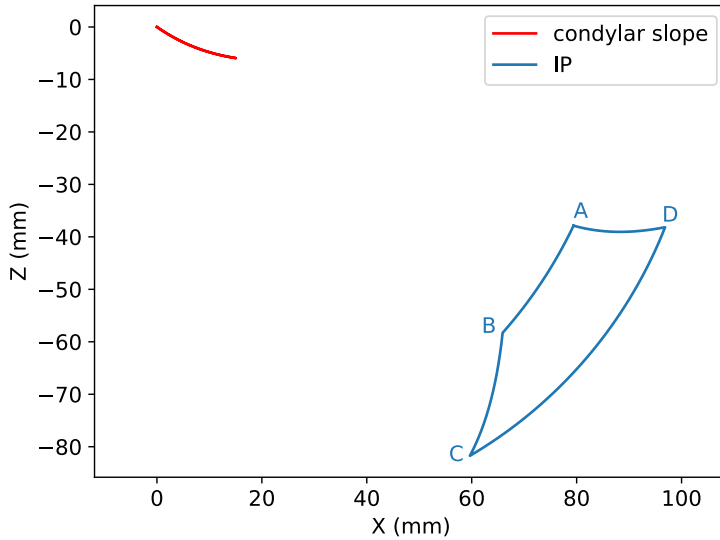
The range of motion of the orthosis must cover that of humans, which is described as Posselt's envelope of motion as shown in Figure 2.3. Boundaries for the parameters of the kinematic model can be defined so that only possible mandible positions can be reached.

Wen et. al [10] used the same kinematic model as described above and proposed boundaries for the transformation parameters so that the movement range covered the Posselt envelope. However, they developed a jaw movement robot for analysing mastication and modelled muscles for controlling the robot movement. The area as defined by the given boundaries, therefore, corresponds to the reachable area of the robot and is larger than that of the human jaw. Nonetheless, these boundaries can be used as a reference for narrowing the reachable area.

The boundary for X is directly given as the horizontal range of movement of the mandible which is 15mm [10]. Due to the correlation of X and Z , the boundary for Z is also defined, as the minimum of the condylar slope. Because the condylar slope and therefore the Z boundary varies from person to person, a more general boundary is used. Leader et al. [29] measured mandible translation and rotation during mouth opening in several subjects. They found the average maximum inferior-superior translation to be 7mm and the average maximum opening rotation to be approximately 34° . These values were used as boundaries for Z and β .

With these boundary values, the Posselt Figure can be reproduced in the sagittal plane, see Figure 5.2. The first segment (from A to B) corresponds to the initial phase of mouth opening and consists of a pure rotation. In this phase, the mouth opens with an inter-incisal distance of approximately 20mm [10]. This distance could be reached by a rotation of $\beta = 16^\circ$ around the condylar axis. Then, protrusion and rotation of the condyles occur simultaneously (segment B to C). In order to reach the maximum opening rotation of 34° , rotation had to be 1.2° for each millimetre of translation. This is plausible in comparison with previous studies on rotation and translation ratio during mouth opening. Depending on the study, this ratio has been reported to be $1.5^\circ/\text{mm}$ [29] or, dependent on condylar slope inclination (from steepest to flattest slope), $2.29^\circ/\text{mm}$, $1.49^\circ/\text{mm}$ and $0.96^\circ/\text{mm}$. The rightmost segment (from C to D) in Figure 5.2 represents the closing movement of the jaw with the condyles at the maximum protrusion. Finally, the upper segment (from D to A) corresponds to the

condyles moving back to their initial position. Contrary to the Posselt Figure 2.3, in Figure 5.2 this segment is a smooth curve because the upper teeth are not taken into consideration in the kinematic model since this does not influence parameter boundaries. The resulting maximum opening distance is 44mm which is less than the expected 50mm. This is due to the relatively flat condylar slope that was used for the kinematic model. An opening distance of 50mm can be reached by using a steeper condylar slope or allowing a larger opening rotation.



	X	β
A	0	0°
B	0	16°
C	15mm	34°
D	15mm	-4°

Figure 5.2.: Envelope of the incisor point in the sagittal plane and the transformation parameters at the characteristic points.

Most studies measuring the displacement of the lower incisors focus on the opening movement while laterotrusion is not evaluated. In one study of masticatory movement, maximum lateral displacement was reported to be 12mm [35]. However, this value was the maximum during mastication, not the maximum possible lateral displacement of the mandible. In a self-conducted test with 5 subjects who were asked to move their jaw sideways as far as possible, values of up to 12mm to one side were measured (equivalent to 24mm of total lateral displacement).

In the kinematic model, Y translation and γ rotation are responsible for lateral displacement of the lower incisors. Y translation corresponds directly to the lateral displacement of the condyles. This movement is very small because the condyles are constrained by bones and ligaments. Most of the lateral movement can therefore be described by a rotation around the Z -axis. With a rotation of 10° , approximately 12mm laterotrusion to one side can be reached. The boundary for γ was set to -10° to 10° which coincides with the respective boundary used for the jaw movement robot [10]. Due to the correlation of α and γ , the boundary for α was also taken from the jaw movement robot. Y was bounded by -2mm to 2mm to allow for a small lateral displacement of the condyles.

Table 5.1 gives an overview of the parameter boundaries.

These boundaries can be refined for a patient-specific movement range.

X	Y	Z	α	β	γ
0–15mm	–2–2mm	–7–0mm	–4–4°	–4–34°	–10–10°

Table 5.1.: Maximum movement range of the instantaneous frame.

5.1.3. Inverse kinematics

For the inverse kinematics, Equation 5.3 is solved for $q = (X, Y, Z, \alpha, \beta, \gamma)^T$, given a target incisor point ${}^M IP_{target}$.

$${}^M IP_{target} = {}^M T_I(q) \cdot {}^I IP \quad (5.3)$$

This equation is solved using a Sequential Least Squares Programming (SLSQP)¹ method with constraints for q as defined in the previous section. The default initial guess for the optimisation is zero for all parameters. When calculating the inverse kinematics for an IP trajectory, the initial guess is set to the result of the optimisation for the previous target IP position.

```
def inverse_kinematics(IP_target):
    # IP_target = mTi(q)*IP_init
    # <=> mTi(q)*IP_init - IP_target = 0
    def fw_kin(q):
        # mTi is the transformation matrix
        # res is a 2d vector of the distances between condylar position and condylar
        # path for left and right condyle
        mTi, res = forward_kinematics_6DOF(q)
        IP = mTi.dot(IP_init)
        err = IP - IP_target
        return np.linalg.norm(res)**2 + np.linalg.norm(err)

    sol = optimize.minimize(fw_kin, initial_q, method="SLSQP",
        bounds=([0, 15], [-5, 5], [-7, 0], [-4, 4], [0, 34], [-10, 10]))

    q = sol.x

    # assert that optimization was successful
    mTi, _, _ = forward_kinematics_6DOF(q)
    error = np.linalg.norm(mTi.dot(inc_init) - inc_target)
    try:
        assert(error < 1e-4) # error margin
    except AssertionError:
        print("target IP was missed by " + str(error) + " mm")

    return q
```

This is an excerpt from the file `kinematic_model.py`.

¹<https://docs.scipy.org/doc/scipy/reference/optimize.minimize-slsqp.html>

5.1.4. Torque calculation

For the application of external forces to the jaw, the torques required to exert those forces can be calculated. They will ultimately be passed as input to the motors of an orthosis.

Torque T in the instantaneous rotation axes is calculated by taking the cross product of the force vector $F = (f_x, f_y, f_z)^T$ and the position vector of the point where the force is applied. Torques applied at the incisor point are determined by the following equation where F is given in mandible coordinates and IP is given with respect to the instantaneous frame:

$$T = {}^IIP \times ({}^M T_I^{-1}(q) \cdot {}^M F) \quad (5.4)$$

As a safety mechanism of the orthosis, applicable force and corresponding torques should have a limit. Maximum bite force at the incisors ranges from 89 to 111 N and at the molar region from 400 to 890 N [6]. Bite forces supplied by the orthosis should not exceed the respective maximum values, i.e. 111 N at the incisors and 890 N at the molars.

The maximum bite force is reached at teeth occlusion and force is enacted from the mandible upon the maxilla. It follows that the force direction can be approximated as the Z-axis of the model. Using the formula given above for the position of the IP and the molars in the biomechanical model, torques for the respective maximum bite forces are calculated, see Table 5.2. They should not be surpassed by the orthosis, and need to be adapted depending on the patient and the required functionality of the orthosis.

$$\text{molar}_{right} = (51.85, -24.80, -32.64)^T, \quad \text{molar}_{left} = (51.85, 24.80, -32.64)^T$$

torque in:	x	y	z
lower incisor	-	-8814.34	-
right molar	-22072	-46146.59	-
left molar	22072	-46146.59	-

Table 5.2.: Torques in Nmm for maximum force biting.

5.2. Therapy routines

Therapy can help the patient regain lost muscle function and a normal range of motion of the jaw. Manual devices are commonly used for treatment, as described in Section 3.1.1, but the results are limited. An active orthosis would allow advanced, personalised therapy and aid neurological rehabilitation. For the orthosis, multiple therapy routines could be implemented and personalised to the patient, using the biomechanical jaw model.

5.2.1. Trajectory following

A therapy routine was developed for helping the patient perform a specific jaw movement. Following a trajectory helps with neurological rehabilitation because it compels the patient to exercise precise control over their jaw muscles. The incisor trace for the movement in a healthy jaw is given, and the patient is supposed to follow this movement. Where the patient cannot reach the desired position, because of compromised muscle function and limited range of motion, the orthosis applies just the right amount of force to reach the desired position.

For this, a PD controller was implemented in Artisynt:

$$f(t) = K_p \cdot e(t) + K_v \cdot (e(t) - e(t_{previous}))/ts, \quad e(t) = x_{is}(t) - x_{target}(t) \quad (5.5)$$

$x_{target}(t)$ is the given trajectory for the IP position for a specific jaw movement and $x_{is}(t)$ is the actual position of the incisor of a patient measured at a time t . ts is the sampling time of the simulation. The resulting force $f(t)$ is the force that needs to be applied at the incisors by the orthosis to follow the trajectory. This force depends on the constants K_p and K_v which determine the effect of the position and the velocity part on the resulting force.

Optimal values for K_p and K_v depend on the specific movement, especially the curvature of the movement, and on how the patient moves the jaw, which can be different in each repetition of the therapy routine. Therefore, in general, there are no optimal values, but they can be approximated for a specific movement and mouth opening range.

5.2.2. Resistance training

Another effective way for training the muscles is by activating them repeatedly against resistance. The orthosis can be programmed so that it provides resistance against the direction in which the jaw is moving. This is especially useful for training the muscles for mouth opening and laterotrusion. Contrary to jaw rehabilitation devices presented in Section 3.1.1, this aims at not only stretching the muscles but training them, which is a huge advantage.

Resistance is applied in the positive Z direction for mouth opening and for left and right laterotrusion respectively in the positive and negative Y direction. The magnitude of the applied force increases with the advancing movement until the externally applied force equals the force exerted by the mandible. When the external force becomes stronger than the force of the mandible, pushing the mandible back, its magnitude is reduced again so that the jaw movement can advance. This results in a balance between the exerted force of the jaw and the externally applied force, where the mandible is always moving against resistance. This is similar to training other muscles in our body with a Deuserband. When the jaw moves back into a resting position, i.e. in the same direction as the resistance force, the externally applied force is reduced to zero because this is not the target training direction.

The force limit is set implicitly because once the force gets too large and starts pushing the jaw in the opposite direction, it is automatically reduced in magnitude. Therefore, the magnitude of the force is determined entirely by the patient and how far they move the mandible. The patient may decide to stop once their pain threshold is reached.

Pseudocode for the implemented algorithm is given below.

5.3. Conclusion

The developed orthosis framework enables the realisation of therapy routines. During therapy, the orthosis supports the jaw movement of a patient by applying external forces on the jaw, specifically at the incisor point. With the developed framework, it is possible to determine the forces that need to be applied by the orthosis to perform a therapy routine. For the application of external forces at the incisor, first, the position and orientation of the orthosis at an instantaneous moment must be determined. This is done by calculating the inverse kinematics for the current incisor position of the patient. Then, forces can be translated to orthosis actuation, i.e. the required torques in the rotation axes of the orthosis. The developed system allows the application of arbitrary forces, therefore jaw rehabilitation can be realised in any direction without limitations. Trajectory following and resistance training therapy routines were proposed, but the system can easily be used for the development of further therapy routines suggested by medical professionals. The orthosis framework can be personalised to the patient by using a patient-specific condylar slope for the kinematic model and by fitting the reachable area of the orthosis to the patient.

In short, based on the ArtiSynth model, the framework provides calculation routines for the forward and inverse kinematics, and a translation of torques to forces, with respect to the defined base coordinate system. These can be used in the software of an orthosis, provided that it has motors for producing torques in three axes, and has two or three prismatic joints which can move with the IP. For implementation details, see <https://github.com/laura-jehn/jaw-modelling-thesis>.

Algorithm 1: Resistance Training Routine

```
Data: IP_position // position of IP
IP_history // list of last 10 IP positions
movementState // one of: IN_MOVEMENT, MOVEMENT_BACK, IDLE or AT_LIMIT
force // resistance currently acting on IP
while  $t < t_{final}$  do
  IP_history.remove(0)
  IP_history.add(IP_position)
  // determine direction to which jaw is moving contrarily
  dir ← IP_history.first – IP_history.last
  velocity ← dir.norm()
  movementThreshold = 0.05 // threshold to determine whether jaw is
  moving
  if velocity < movementThreshold then
    // jaw is not moving
    switch movementState do
      case IN_MOVEMENT do
        // jaw has reached limit movement
        movementState ← AT_LIMIT
        // decrement force magnitude
        force.magnitude – = 1
      end
      case MOVEMENT_BACK do
        // jaw was in backward movement and has now come to rest
        movementState ← IDLE
      end
    end
  else
    // jaw is moving, determine whether it is moving in training
    direction
    if  $-1 \cdot \text{sign} \cdot \text{dir.axis} / \text{dir.norm}() > 0.85$  then
      // jaw is moving against the resistance, increment force
      magnitude
      movementState ← IN_MOVEMENT
      force.magnitude + = 1
      // set force direction to 1 or -1 in movement axis
      force.direction.axis ←  $-1 \cdot \text{sign}$ 
    else
      // jaw is moving contrary to training direction, decrement
      force magnitude
      movementState ← MOVEMENT_BACK
      force.magnitude – = 1
    end
  end
end
end
```

6. Evaluation

In this chapter, the developed orthosis framework is evaluated, including an evaluation of the kinematic model, and its application in the context of therapy routines, as developed in Chapter 5. Therapy is simulated on a model of the jaw with reduced muscle forces and a limited range of motion as presented in Chapter 4.

6.1. Evaluation of the kinematic model

The kinematic model was evaluated for mouth opening and mastication. Each of these movements was performed with the biomechanical model in ArtiSynth and the movement of the lower incisor point (IP) tracked. The inverse kinematics were calculated for the resulting IP trajectory of the two movements. Using the forward kinematics for the solution of the inverse kinematics, the positions of the original IP and the calculated IP were compared. For all IP positions in the chewing and opening movement, this error was smaller than 10^{-4} mm. It follows that rotation and translation parameters can be found for reaching a target IP position with a precision of 10^{-4} mm. Beyond reaching the target IP position, the rotation and translation parameters are also relevant. The inverse kinematics solution is ambiguous, for example, if the target IP position can be reached with pure translations, and with a combination of rotations and translations. Ideally, the found solution should correspond to the actual rotation and translation of the mandible when the incisor is at the target position. In general, the same incisor position can be reached with different mandibular movement, similar to the ambiguity of the inverse kinematics. However, for a mouth opening and chewing movement, the rotation and translation of the mandible during the movement is described in literature and will be compared to the transformation parameters of the kinematic model.

Furthermore, the transformation parameters of the model can be compared to the internal transformation in ArtiSynth. The position of the instantaneous frame at the centre of the condylar axis is not part of the rigid body modelling the jaw and, therefore, its rotation and translation are not inherently calculated in the simulation. However, a rotation is given at the lower incisors, corresponding to the internal rotation of the mandible, and can be used for a comparison to the frame rotation of the kinematic model. For a comparison of the translations, the displacement of the midpoint of the condylar axis can be calculated in the simulation.

For the validity of the comparison, the kinematic model used the original condylar slope of the biomechanical model without personalisation, taken from ArtiSynth:

$$Z = -0.0003X^3 + 0.0247X^2 - 0.6981X$$

6.1.1. Mouth opening

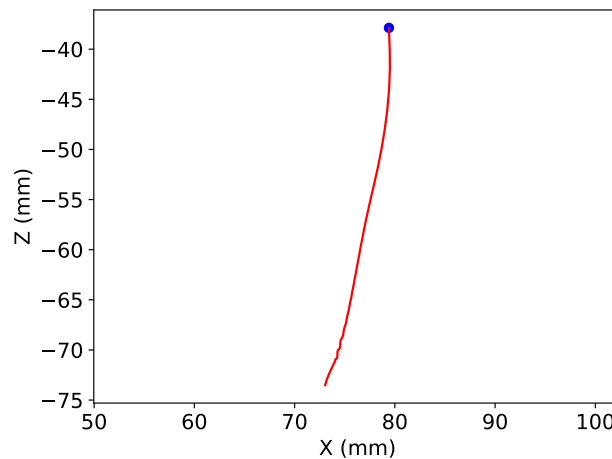


Figure 6.1.: IP trajectory during mouth opening in the sagittal plane.

Figure 6.1 shows the trajectory of the IP during maximum mouth opening in the simulation. The transformation parameters for the mandible to reach this incisor trajectory are shown in Figure 6.2. Only translation in x and z, and rotation around the y-axis were significant, all other parameters were negligible since they were smaller than 0.005mm or 0.005°. Frame translation (the left plot of Figure 6.2) describes the condylar slope. This corresponds to the mouth opening movement as reported in literature: a protrusion of the condyles along the condylar slope and an opening rotation of the condyles.

In a comparison with the internal transformation of the mandible in Artisynt, see Figure 6.2, it can be noted that the transformation parameters were almost identical. The average absolute error for frame translation was 0.09mm, with a maximum error of 0.16mm. For frame rotation the average error was 0.06°, with a maximum error of 0.11°.

In the simulation, the condyles protruded 16mm during the maximum mouth opening. This is further than the 15mm which were set as a boundary for the x-translation in the kinematic model, cf. 5.1. In the simulation, the protrusion of the condyles is constrained by the length and activation of the opening muscles but there are no ligaments or other structures constraining the condyles. As a result, when the opening muscles are maximally activated, the condyles can protrude further than anatomically possible. To take this into account, the boundary for the x-translation in the kinematic model was set to 16mm, so that all target IP positions for the simulated movement were within the reachable area of the kinematic model.

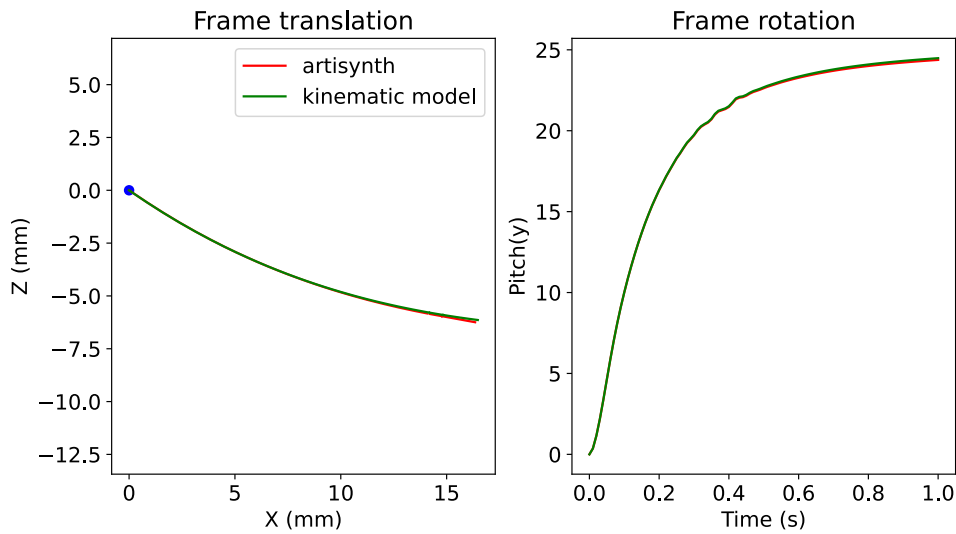


Figure 6.2.: Comparison of rotation and translation of the instantaneous frame during mouth opening.

6.1.2. Mastication

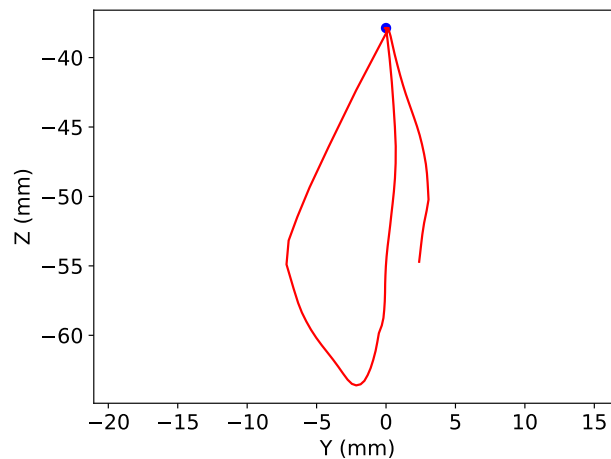


Figure 6.3.: IP trajectory during chewing in the frontal plane.

The trajectory of the IP during the simulated chewing is plotted in Figure 6.3. Transformation parameters for the mandible to reach the incisor trajectory are shown in Figure 6.4. Again, frame translation is only in the x and z-direction, but unlike during mouth opening, there is a significant rotation in all three axes. In the plot for frame rotation, three segments can be identified. The first 0.5 seconds correspond to one chewing cycle. Then, the mouth is closed for 0.3 seconds where all rotations are zero before another chewing cycle starts. This behaviour matches analyses of mastication in literature which report that lateral deviation of the mandible is caused by rotations

while the lateral displacement of the condyles is almost non-existent. It follows that mastication is also accurately described by the kinematic model.

Comparing frame translation and rotation with the simulation shows that the transformation parameters are very similar, especially rotation in y is identical, see Figure 6.4. It can be noted that rotation in x and z are slightly larger in the simulation than in the kinematic model, but the curves are similar in shape. In total, the average absolute error for frame rotation was 0.38° with a maximum of 1.16° . There are also small differences in frame translation, on average 0.65mm, and a maximum difference of 2.16mm, which explain the difference in rotation magnitude. Although bigger than for mouth opening, these errors are still small.

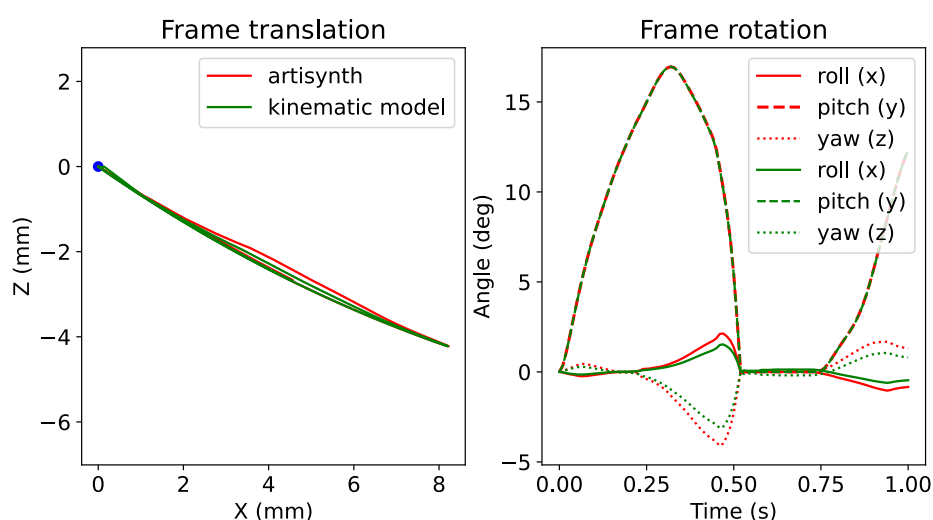


Figure 6.4.: Comparison of rotation and translation of the instantaneous frame during chewing.

6.1.3. Torque calculation

For an evaluation of the torque calculation, torques are calculated for forces applied at the incisor point during mouth opening and chewing. The forces used for evaluation were 1 N in x, y and z-direction of the static mandible frame and the torques were calculated as torques in the axes of the instantaneous frame in Nmm. The results were compared to torque calculation in ArtiSynth which had already been implemented.

Figures 6.5 and 6.6 show that torque calculation for the kinematic model and in the simulation are the same. Differences between the graphs are due to the differences in frame translation and rotation described in the previous sections. It follows that torques are calculated correctly.

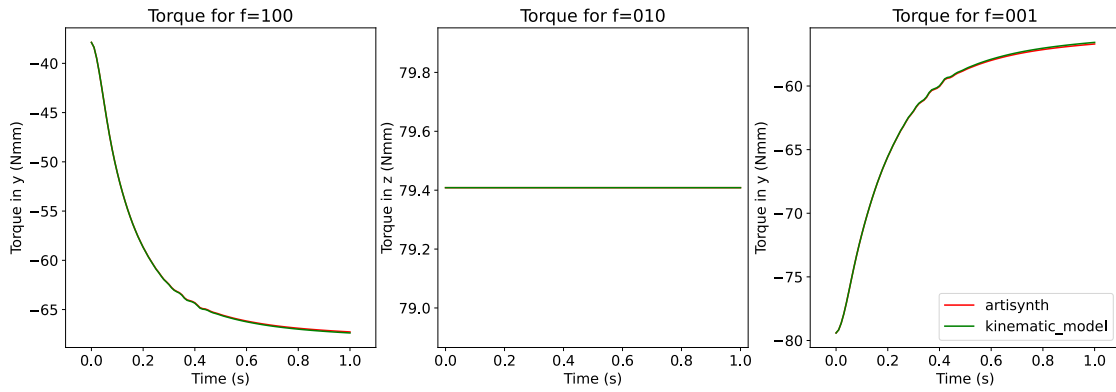


Figure 6.5.: Comparison of calculated torques during mouth opening for sample forces.

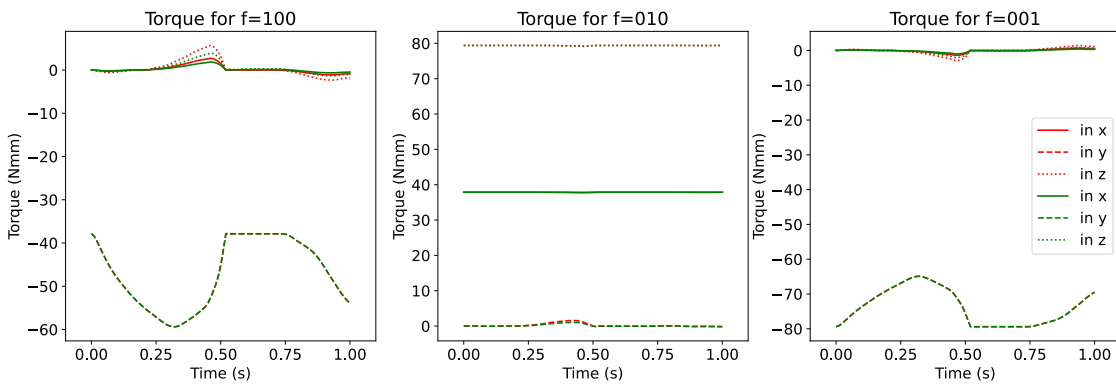


Figure 6.6.: Comparison of calculated torques during chewing for sample forces.

6.2. Evaluation of the trajectory following

The controller was evaluated for the chewing movement. For this, the IP trace of the biomechanical jaw model was captured during chewing with full muscle function. In order to test the therapy routine on a jaw with compromised muscle function, the biomechanical model was adjusted accordingly. The maximum muscle forces of the mouth opening muscles were reduced to 20% of the force. Figure 6.7 shows the effect this has on the chewing movement.

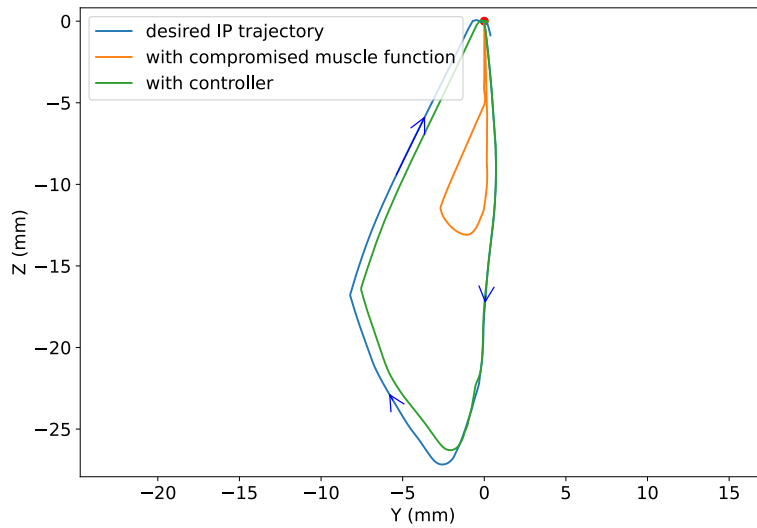


Figure 6.7.: IP trajectory during chewing in the frontal plane in three scenarios: With full muscle function (blue), with maximum muscle force of the opening muscles reduced to 20% (yellow), with externally applied forces (green).

For determining K_p and K_v , the root mean square error, as defined in Equation 6.1, is calculated. This error should be small and the trajectory of the calculated force should be smooth.

$$error = \sqrt{\frac{\sum_{t=0}^{t_{final}} (x_{is}(t) - x_{target}(t))^2}{t_{final}/t_{step}}} \quad (6.1)$$

The error was evaluated for varying K_p and K_v , as shown in Figure 6.8. In general, the error decreases for higher values of K_p , however, if K_v is too small, the error increases dramatically with a larger K_p .

Figure 6.9 shows the calculated forces for $K_p = 15$ and $K_v = 0, 0.005, 0.02, 0.05$. For $K_v = 0$ there are strong oscillations. Oscillating force trajectories are not a problem for the simulation, but they become a problem for the orthosis because it has to change the direction of the force quickly which can lead to instability. The curve is smoother for a higher value of K_v , however, the oscillations

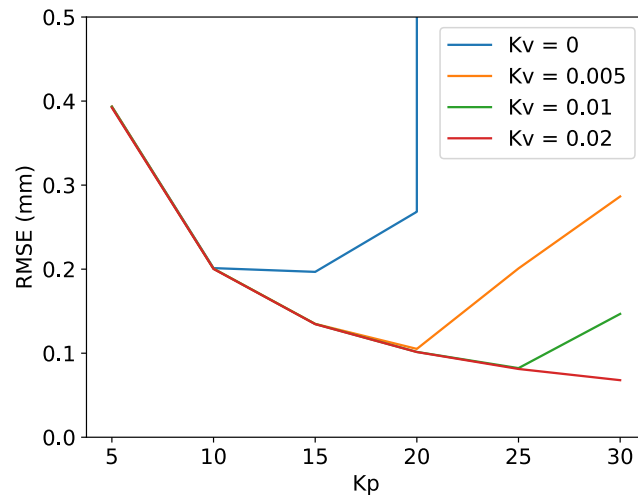


Figure 6.8.: Root mean square error for different values of K_p and K_v .

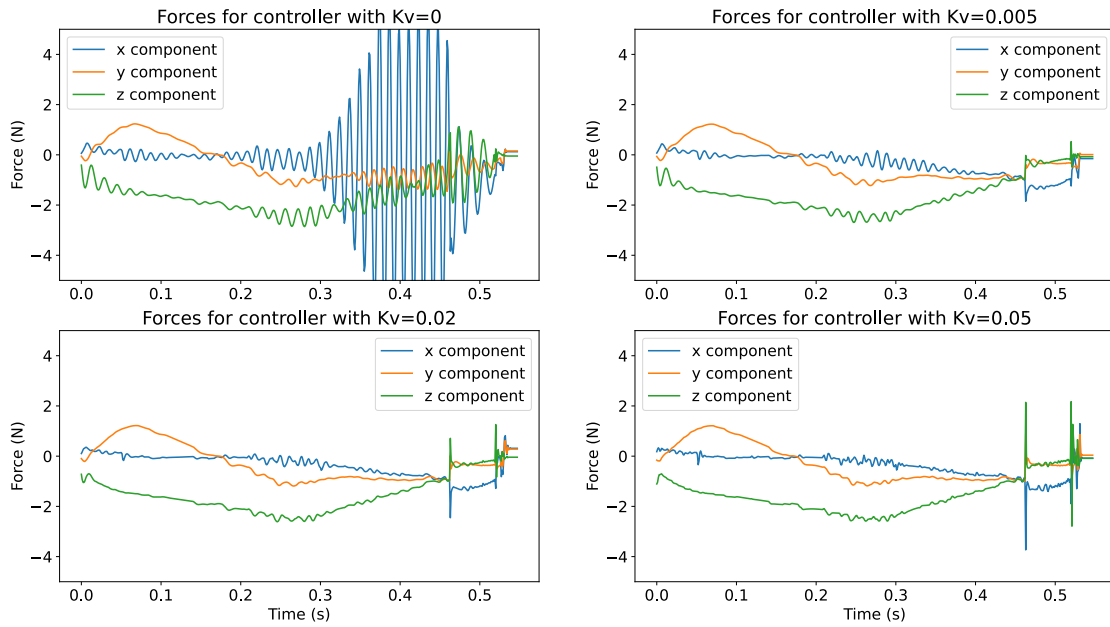


Figure 6.9.: Controller forces for $K_p = 15$ and $K_v = 0, 0.005, 0.02, 0.05$.

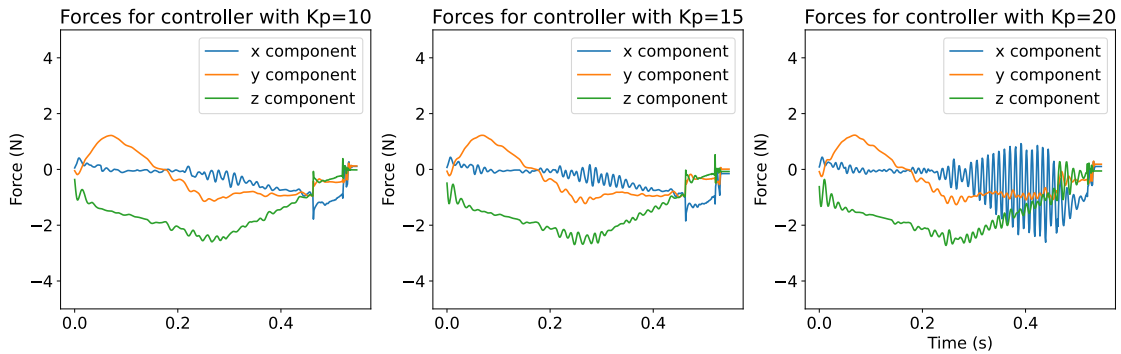


Figure 6.10.: Controller forces for $K_v = 0.005$ and $K_p = 10, 15, 20$.

at $t = 0.45$ also increase. Here, the closing of the mouth begins. Oscillations occur because this movement happens very quickly.

In Figure 6.10 the control forces are plotted for $K_v = 0.005$ and $K_p = 10, 15, 20$. For $K_p = 20$, there are strong oscillations while for $K_p = 10$ and 15 almost no difference can be noted.

As a good compromise between a smooth force trajectory and a small error, $K_v = 0.005$ and $K_p = 15$ were chosen. The resulting error is small and the trajectory is followed closely, see Figure 6.7. The resulting incisor movement is caused partially by muscle activation and partially by forces externally applied to the jaw.

Some observations can be made from Figure 6.10. The negative z-component of the force represents that the orthosis assists with mouth opening. There is also a notable y-component which stands for the assistance with lateral motion of the jaw.

The stability of the applied forces is important when translating them to corresponding torques. If the trajectory of the force is unstable, then so is the trajectory of the torque that needs to be applied by the orthosis to produce this force. For $K_p = 15$ and $K_v = 0.005$, the torques needed to produce the desired force were plotted in Figure 6.11. For torque calculation, the mandible's rotation was determined using the inverse kinematics for the controlled IP trajectory.

6.3. Evaluation of the resistance training

For an evaluation of the resistance training routine, mouth opening and laterotrusion were simulated and the forces were calculated, visualised and translated to torques in the instantaneous rotation axes. For representing TMD in the simulation, the maximum muscle force of the opening muscles was set to 20% so that the mouth opening range was limited.

Figure 6.12 shows the results for the mouth opening movement in three scenarios: with compromised muscle function as described above (i.e. reduced to 20% of the original force), with full muscle function and for only activating the muscles 50% of their maximum activation. In the first scenario, with compromised muscle function, the maximum applied force was 4 N. With full muscle function,

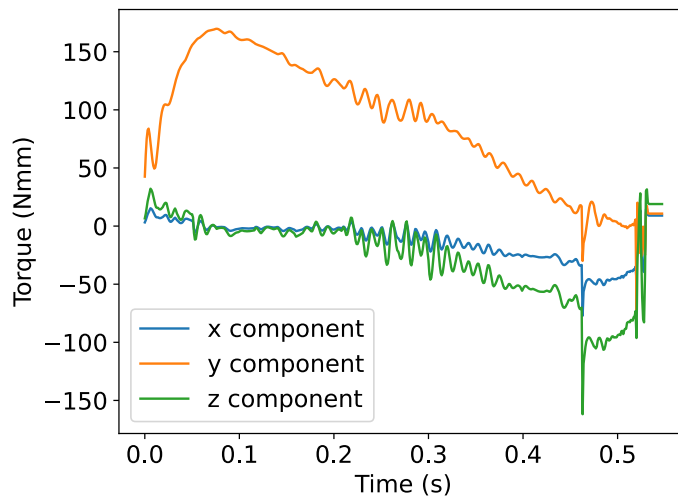


Figure 6.11.: Torques for producing controller force given in Figure 6.10.

the maximum applied force rises to over 6 N. If the muscles are only activated halfway, a maximum force of 3 N is applied. This implies that muscle activation and exerted force during mouth opening against resistance are not proportional, at 50% of the muscle activation, 75% of the force exerted by the jaw remains. The same goes for maximum muscle forces, even when reduced to 20% of their original force, $\frac{2}{3}$ of the force exerted by the jaw remains.

The oscillations in the curves are due to the increment of muscle activation and resistance force. For mouth opening, the force is incremented by 0.05 Newton every time step and the activation of the mouth opening muscles by 0.0025 Newton. In training with a real patient, the activation of the mouth opening muscles will be continuous, reducing oscillations. With smaller time steps and lower increments, the oscillations can also be reduced. However, with a smaller increment of the force, it would take longer to reach maximum resistance and the patient would have to keep their mouth open for a longer time. At $t = 3.5s$ the closing movement begins, and the force goes to zero. In the right plot of the figure, torques are plotted for the resistance training with compromised muscle function.

Figure 6.13 shows the results for the left laterotrusion movement. Laterotrusion is caused by activating the inferior pterygoid muscle on one side. This muscle belongs to the opening muscles and, therefore, its maximum force was reduced to 20% in this simulation. As a result, the maximum applied force was only 1 N because the mandible cannot produce a large lateral force. Again, at $t = 4s$ the movement back into a resting position begins, and the force goes to zero. Small oscillations can be observed due to the increase and decrease of the force magnitude by 0.01 N each time step. Even though this value is small, it causes oscillations because the total exertable force during laterotrusion is only 1 N and therefore even a difference of 0.01 N can have an effect on the direction in which the mandible is moving. For producing a force in y-direction, torques have to be applied both in the x and z-axis.

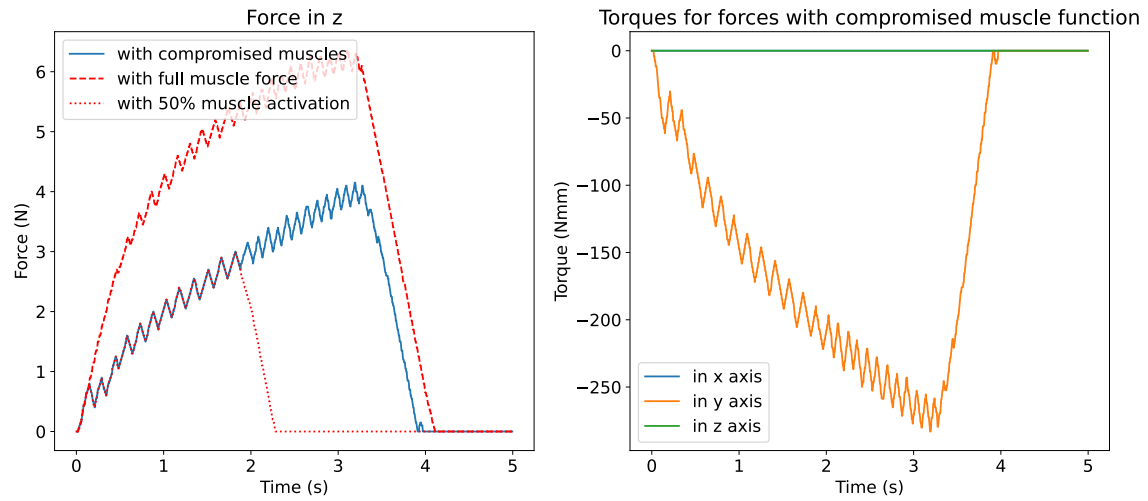


Figure 6.12.: Forces and torques for exerting resistance during a mouth opening movement.

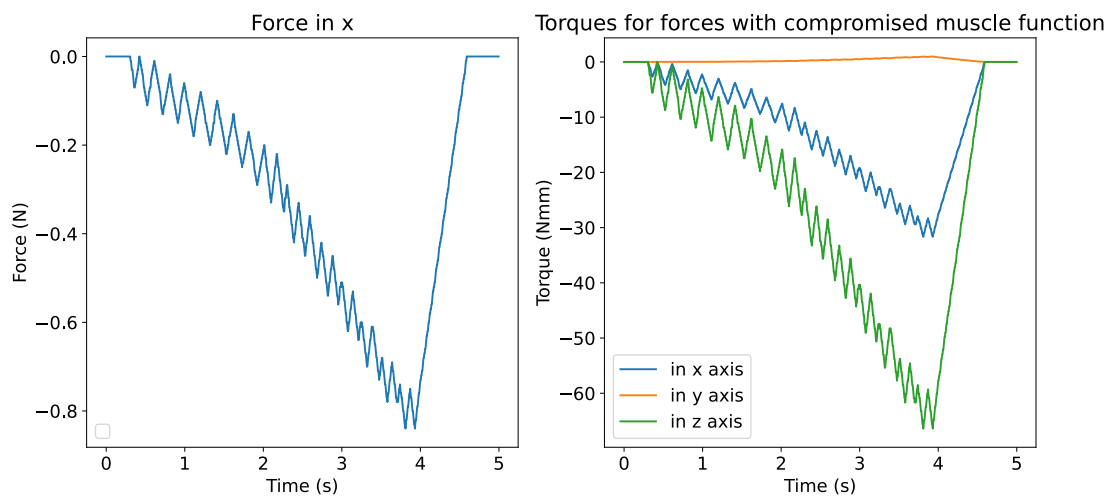


Figure 6.13.: Forces and torques for exerting resistance during a left laterotrusion movement.

6.4. Conclusion

It was shown that the kinematic model accurately describes mandibular motion and enables the translation of forces applied at the jaw to torques in the instantaneous rotation axes of the orthosis. Using the orthosis framework, trajectory following can be performed, and with the biomechanical model, the parameters for the trajectory following can be determined. The orthosis can help a patient who, on their own, can only perform a limited chewing movement, perform the full movement. It is also possible to use the orthosis to perform resistance training during mouth opening and laterotrusion movements, for a strengthening of the muscles.

While this demonstrates the various capabilities of the developed framework, the complexity of the system could present a challenge because the technical implementation requires at least 4-DOF. Furthermore, the framework was designed for the application of forces at the incisors only, as this was the case for many existing jaw rehabilitation devices, but it might become useful, for other therapy routines, to make this location on the mandible interchangeable. Another aspect that was not addressed by the orthosis framework is the integration of a patient's pain limit which should, in practice, limit the forces applied on the jaw. This presents a limitation of the framework. In general, the developed therapy was based on the ArtiSynth model, and, therefore, depends on the accuracy and simulation quality of this model. For jaw movements, only limited data is available, for example, the model provides only one sample input probe with muscle activations for a chewing movement.

7. Conclusion and Future Work

In this thesis, a framework for the development of an orthosis was developed, that expands an existing jaw model with personalisations and TMD symptoms, enabling personalised TMD treatment.

The developed jaw model, based on the existing jaw model in ArtiSynth, allows for personalisation of the condylar slope. Common TMD symptoms, specifically limited bite force and a limited range of motion, can be represented in the model, making it possible to use the model for the development of therapy routines specifically targeting these TMD symptoms. Jaw personalisation was not evaluated with patient data due to lack thereof. This should be covered in future work. Data is required for patients with TMD and should include maximum bite force, maximum mouth opening distance, condylar slope or slope inclination. The model can then be personalised according to this data and the resulting jaw movement can be compared to that of the patient.

For the inclusion of disk-related TMDs in the model, it should be extended with the articular disks. While the disk was modelled statically in this work, some difficulties remain with a dynamic simulation of the disk, due to numerical instability of the FEM. This issue still needs to be addressed and disk-related TMDs should be modelled in future work.

As for the developed orthosis framework, it can be personalised to the patient by using a patient-specific condylar slope for the kinematic model and by fitting the reachable area of the orthosis to the patient. The framework consists of a kinematic model for describing the range of motion of the orthosis, and the translation of external forces, acting on the jaw as part of a therapy routine, to orthosis actuation. The orthosis has 4-DOF and allows for the application of arbitrary forces, provided that it has motors for producing torques in three axes, and has at least two prismatic joints which can move with the IP. Thus, jaw rehabilitation in any direction can be supported. Implemented therapy routines for the orthosis were trajectory following and resistance training. With the trajectory following routine, the orthosis can, for example, help a patient who, on their own, can only perform a limited chewing movement, perform the full movement, whereas resistance training helps strengthen the muscles. The provided therapy can be personalised to the patient in terms of the range of motion and difficulty level.

The system offers the possibility to develop further therapy routines with little effort, allowing the capabilities of the orthosis to be continuously and easily expanded. As a result, this offers more flexibility in treatment options than currently available.

Finally, the design of an orthosis that implements the concepts developed in this work should be addressed in future work.

Bibliography

- [1] R. Akhter. “Epidemiology of Temporomandibular Disorder in the General Population: a Systematic Review”. In: *Advances in Dentistry & Oral Health* 10 (Feb. 2019). doi: 10.19080/ADOH.2019.10.555787.
- [2] W.R. Martins et al. “Efficacy of musculoskeletal manual approach in the treatment of temporomandibular joint disorder: A systematic review with meta-analysis”. In: *Manual Therapy* 21 (2016), pp. 10–17. doi: 10.1016/j.math.2015.06.009.
- [3] S. Ingawale and T. Goswami. “Biomechanics of the Temporomandibular Joint”. In: *Human Musculoskeletal Biomechanics*. Jan. 2012. doi: 10.5772/33702.
- [4] S.R. Suppelt. “Measurement Setup to Support the Diagnosis of Temporomandibular Disorders”. Unpublished. MA thesis. Dept. of ETiT, Technical University of Darmstadt, Darmstadt, Germany, Apr. 2021.
- [5] S.J. Scrivani, D.A. Keith, and L.B. Kaban. “Temporomandibular disorders”. In: *The New England journal of medicine* 359.25 (2008). doi: 10.1056/NEJMra0802472.
- [6] K.J. Anusavice et al. *Phillips’ science of dental materials*. Elsevier/Saunders, 2013, p. 67.
- [7] I. Stavness et al. *An Integrated Dynamic Jaw and Laryngeal Model Constructed from CT Data*. 2006.
- [8] K. Koter and P. Žak. *A Novel Automated Device for Jaw Rehabilitation*. 2020.
- [9] U. Posselt. *Studies in the mobility of the human mandible*. Copenhagen, 1952.
- [10] H. Wen, P. Xu, and M. Cong. “Kinematic Model and Analysis of an Actuation Redundant Parallel Robot With Higher Kinematic Pairs for Jaw Movement”. In: *IEEE Transactions on Industrial Electronics* 62 (Mar. 2015), pp. 1590–1598. doi: 10.1109/TIE.2014.2365432.
- [11] R. Lee et al. “Randomised feasibility study to compare the use of Therabite with wooden spatulas to relieve and prevent trismus in patients with cancer of the head and neck”. In: *British Journal of Oral and Maxillofacial Surgery* 56.4 (2018), pp. 283–291. doi: 10.1016/j.bjoms.2018.02.012.
- [12] A. Singh et al. “Intricate role of trismus appliance in dental perspectives: A comprehensive cum technical revelation”. In: *International Journal of Oral Health and Medical Research* 2.6 (2016), pp. 98–100.
- [13] B. Thiagarajan. “Trismus an overview”. In: *ENT SCHOLAR* (June 2014).

-
- [14] “Therabite jaw motion rehabilitation system.” In: *Atmos Medical* (2009). url: <https://www.atosmedical.co.uk/product/therabite-jaw-motion-rehabilitation-system/>.
- [15] H. Takanobu et al. “Mouth Opening and Closing Training with 6-DOF Parallel Robot.” In: *Proceedings - IEEE International Conference on Robotics and Automation 2* (Jan. 2000), pp. 1384–1389. doi: 10.1109/ROBOT.2000.844791.
- [16] M. Evans et al. “A shoulder-mounted robotic exoskeleton for rehabilitation of temporomandibular disorder via assisted motion of the jaw”. In: *2016 IEEE 14th International Workshop on Advanced Motion Control (AMC)*. 2016, pp. 30–37. doi: 10.1109/AMC.2016.7496324.
- [17] S. Surya et al. “Robotic exoskeleton for rehabilitation of TMD via assisted motion of jaw”. In: *2017 International Conference on Inventive Communication and Computational Technologies (ICICCT)*. 2017, pp. 172–177. doi: 10.1109/ICICCT.2017.7975182.
- [18] J.H. Koolstra and T.M.G.J. van Eijden. “The jaw open-close movements predicted by biomechanical modelling”. In: *Journal of Biomechanics* 30.9 (1997), pp. 943–950. doi: 10.1016/S0021-9290(97)00058-4.
- [19] C.C. Peck, G.E.J. Langenbach, and A.G. Hannam. “Dynamic simulation of muscle and articular properties during human wide jaw opening”. In: *Archives of Oral Biology* 45.11 (2000), pp. 963–982. doi: 10.1016/S0003-9969(00)00071-6.
- [20] A.V. Hill. “The mechanics of active muscle”. In: *Proceedings of the Royal Society of London. Series B, Biological sciences* 141,902 (1953), pp. 104–117. doi: 10.1098/rspb.1953.0027.
- [21] C.C. Peck and A.G. Hannam. *Human jaw and muscle modelling*. 2006.
- [22] J.E. Lloyd, I. Stavness, and S. Fels. “ArtiSynth: A Fast Interactive Biomechanical Modeling Toolkit Combining Multibody and Finite Element Simulation”. In: *Soft Tissue Biomechanical Modeling for Computer Assisted Surgery*. Springer, 2012, pp. 355–394. url: www.artisynth.org.
- [23] D.C. Ackland et al. “A personalized 3D-printed prosthetic joint replacement for the human temporomandibular joint: From implant design to implantation”. In: *Journal of the Mechanical Behavior of Biomedical Materials* 69 (2017), pp. 404–411. doi: 10.1016/j.jmbbm.2017.01.048.
- [24] J.H. Koolstra and T.M.G.J. van Eijden. *Combined finite-element and rigid-body analysis of human jaw joint dynamics*. 2005. doi: 10.1016/j.jbiomech.2004.10.014.
- [25] B. Sagl et al. “A Dynamic Jaw Model With a Finite-Element Temporomandibular Joint”. In: *Frontiers in Physiology* 10 (2019), p. 1156. doi: 10.3389/fphys.2019.01156.
- [26] M. Skipper Andersen et al. “Introduction to Force-Dependent Kinematics: Theory and Application to Mandible Modeling”. In: *Journal of biomechanical engineering* 139.9 (2017). doi: 10.1115/1.4037100.
- [27] S.E. Martinez Choy et al. “Realistic kinetic loading of the jaw system during single chewing cycles: a finite element study”. In: *Journal of Oral Rehabilitation* 44.5 (2017), pp. 375–384. doi: 10.1111/joor.12501.

-
- [28] T. Weingärtner, S. Hassfeld, and R. Dillmann. “Dynamic Simulation of the Jaw and Chewing Muscles for Maxillofacial Surgery”. In: *Proceedings IEEE Nonrigid and Articulated Motion Workshop*. July 1997, pp. 104–111. doi: 10.1109/NAMW.1997.609860.
- [29] J.K. Leader et al. “Mandibular kinematics represented by a non-orthogonal floating axis joint coordinate system”. In: *Journal of Biomechanics* 36.2 (2003), pp. 275–281. doi: 10.1016/S0021-9290(02)00337-8.
- [30] S.J. Ahn et al. “Analyzing center of rotation during opening and closing movements of the mandible using computer simulations”. In: *Journal of Biomechanics* 48.4 (2015), pp. 666–671. doi: 10.1016/j.jbiomech.2014.12.041.
- [31] P.U. Dijkstra et al. “Angle of mouth opening measurement: realibility of a technique for temporomandibular joint mobility assessment”. In: *Journal of Oral Rehabilitation* 22.4 (1995), pp. 263–268. doi: 10.1111/j.1365-2842.1995.tb00084.x.
- [32] J. Coutant et al. “Temporo Mandibular Joint Kinematic: The Specificity of the Rotatory Component Involved in Disc-Condyle Displacements along the Temporal Bone Surface”. In: *IFMBE Proceedings* 37 (Jan. 2011), pp. 799–802. doi: 10.1007/978-3-642-23508-5_208.
- [33] F. Cordray. “The Relationship between Occlusion and TMD”. In: *Open Journal of Stomatology* 07 (Jan. 2017), pp. 35–80. doi: 10.4236/ojst.2017.71003.
- [34] A. Okino et al. “A Clinical Jaw Movement Training Robot for Lateral Movement Training.” In: *2003 IEEE International Conference on Robotics and Automation (Cat. No.03CH37422)*. Vol. 1. Oct. 2003, 244–249 vol.1. doi: 10.1109/ROBOT.2003.1241603.
- [35] T. Ogawa, M. Ogawa, and K. Koyano. “Different responses of masticatory movements after alteration of occlusal guidance related to individual movement pattern”. In: *Journal of oral rehabilitation* 28 (Sept. 2001), pp. 830–41. doi: 10.1111/j.1365-2842.2001.00672.x.



A. Appendix

List of Figures

2.1. Anatomy of the TMJ. Adopted from [3].	3
2.2. Muscles associated with jaw function. [4]	4
2.3. Posselt figure: Maximal envelope that the lower IP can reach in (a) transverse plane and (b) sagittal plane [10].	5
3.1. Insertion based rehabilitation devices [8]	7
3.2. 6-DOF Parallel Robot WY-5 [15]	8
3.3. A Novel Automated Device [8]	8
3.4. Exoskeletons	9
3.5. Stavness et al., 2006 [7]	10
3.6. Koolstra and van Eijden, 2005 [24]	10
3.7. A kinematic model with three revolute joints. [28]	12
3.8. Orientation of the non-orthogonal floating axis joint coordinate system. [29]	13
3.9. 4-DOF mandibular motion [10]	14
3.10. ICRs during opening movement is represented by blue points, while red points show ICRs during closing. [30]	15
4.1. Creation of a FEM of the articular disk.	19
4.2. Illustration of the parameters defining the condylar slope.	20
4.3. Approximation of the condylar slope for different slope characteristics.	21
4.4. IP trace during mouth opening-closing for the condylar slopes given in Figure 4.3, in the sagittal plane.	22
4.5. Correlation between reduced maximum muscle force and maximum mouth opening distance and muscle activation and opening distance.	23
4.6. Correlation between reduced maximum muscle forces and maximum bite force in the molar region at different opening distances.	24
5.1. Degrees of freedom of the mandible. [15]	26
5.2. Envelope of the incisor point in the sagittal plane and the transformation parameters at the characteristic points.	29
6.1. IP trajectory during mouth opening in the sagittal plane.	36
6.2. Comparison of rotation and translation of the instantaneous frame during mouth opening.	37
6.3. IP trajectory during chewing in the frontal plane.	37

6.4. Comparison of rotation and translation of the instantaneous frame during chewing. .	38
6.5. Comparison of calculated torques during mouth opening for sample forces.	39
6.6. Comparison of calculated torques during chewing for sample forces.	39
6.7. IP trajectory during chewing in the frontal plane in three scenarios: With full muscle function (blue), with maximum muscle force of the opening muscles reduced to 20% (yellow), with externally applied forces (green).	40
6.8. Root mean square error for different values of K_p and K_v	41
6.9. Controller forces for $K_p = 15$ and $K_v = 0, 0.005, 0.02, 0.05$	41
6.10. Controller forces for $K_v = 0.005$ and $K_p = 10, 15, 20$	42
6.11. Torques for producing controller force given in Figure 6.10.	43
6.12. Forces and torques for exerting resistance during a mouth opening movement. . . .	44
6.13. Forces and torques for exerting resistance during a left laterotrusion movement. . . .	44
A.1. Inverted elements visualised in MeshLab.	64



List of Tables

2.1. Functional muscle groups for mouth opening, closing and laterotrusion [7].	5
5.1. Maximum movement range of the instantaneous frame.	30
5.2. Torques in Nmm for maximum force biting.	31

A.1. Code structure

The code structure and some of the main classes and scripts are given below, however, for a more detailed insight into the written code, the reader is invited to have a look at the GitHub repository <https://github.com/laura-jehn/jaw-modelling-thesis>. Instructions for executing and modifying the code can be found in the repository.

In the class `JawModel`, the jaw is modelled, while `JawDemo` instantiates the model and performs a dynamic simulation. Both classes already existed in `ArtiSynth` and were modified as described in the previous chapters. `artisyntn_models/` as well as `dynjaw/` contain more files, but they are not relevant for this work. The script `python_scripts/kinematic_model_evaluation.py` contains examples for using the kinematic model.

```
/
├── condyleSurface.obj ..... surface mesh of condyle for extrusion
├── saveMarkerPositions.py .....see A.2.1
├── trajectoryFollowing.py .....see A.2.2
├── resistanceTraining.py ..... see A.2.3
├── artisyntn_models/ ..... external models
│   ├── .../dynjaw/ ..... directory for jaw models
│   │   ├── JawModel.java ..... pre-existing jaw model
│   │   ├── JawDemo.java ..... defines dynamic simulation of the jaw model
│   │   ├── ResistanceTraining.java
│   │   ├── TrajectoryFollowing.java
│   │   ├── TorqueDemo.java .....determines transformation of the mandible
│   │   └── FEMDisk.java ..... models of the articular disk
├── python_scripts/
│   ├── data_files/ .....contains data files used for plotting
│   │   └── ...
│   ├── kinematic_model.py
│   ├── kinematic_model_evaluation.py
│   ├── plot_posselt.py ..... plots the posselt envelope using the kinematic model
│   ├── plot_limited_ROM.py .....plots for Section 4.3
│   ├── plot_condylar_slopes_IP_trace.py
│   ├── resistance_training_plots.py
│   ├── trajectory_following_plots.py
│   ├── plot_control_error.py
│   └── plot_chewing_IP_trace.py ..... plots Figure 6.7
```

A.2. Interfacing ArtiSynth with Jython

A.2.1. Basics

The following script `saveMarkerPositions.py` demonstrates how to run a simulation from Jython. It is used for saving the trajectory of the incisors, condyles or other model elements during a simulation run to a file.

```
# ArtisyntScript: "saveMarkerPositions"

loadModel('artisynt.models.dynjaw.<Class>') # substitute <Class> with class name of
                                           model

jawModel =find("models/jawmodel") # get jaw model

ltmj =find("models/jawmodel/frameMarkers/ltmj") # get model element
rtmj =find("models/jawmodel/frameMarkers/rtmj")
lowerIncisor =find("models/jawmodel/frameMarkers/lowerincisor")
upperIncisor =find("models/jawmodel/frameMarkers/upperincisor")

rCondyleTrace =open('../data/rtmjTrace.txt', 'w')
lCondyleTrace =open('../data/ltmjTrace.txt', 'w')
lowerIncisorTrace =open('../data/liTrace.txt', 'w')

play() # start simulation

while getTime()<2: # stop after 2 seconds
    rCondyleTrace.write(rtmj.getPosition().toString() +'\n') # get rtmj position and
                                                            write to file
    lCondyleTrace.write(ltmj.getPosition().toString() +'\n')
    lowerIncisorTrace.write(lowerIncisor.getPosition().toString() +'\n')
    step() # advance simulation by one time step

lCondyleTrace.close()
rCondyleTrace.close()
lowerIncisorTrace.close()

quit() # close simulation
```

A.2.2. Setting control parameters for trajectory following

The script `trajectoryFollowing.py` was used for starting the trajectory following simulation with different K_v and K_p values and saving the error to a file.

```
# ArtisyntScript: "trajectoryFollowing"

loadModel('artisynt.models.dynjaw.TrajectoryFollowing')
```

```

m =root()

Kv =[0, 0.005, 0.01, 0.02]

for kv in Kv:
    f_name = '../python_scripts/data_files/x_error_' +str(kv) +'.txt'
    out_error =open(f_name, 'w')
    m.setKv(kv)
    for kp in range(5, 31, 5):
        m.setKp(kp)
        while getTime()<0.55:
            step()
        err =m.getXError()
        out_error.write(str(kp) + " " +str(err) +"\n")
        m.resetXError()
        reset() # resets simulation
        print("run: "+ str(kp) +", " +str(kv))
        print(err)
    out_error.close()

quit()

```

A.2.3. Setting mode for resistance training

The script `resistanceTraining.py` was used for

```

# ArtisyntScript: "resistanceTraining"

loadModel('artisynt.models.dynjaw.ResistanceTraining')
m =root()

trainingList =[m.TrainingType.OPENING, m.TrainingType.LEFT_LATEROTRUSION,
               m.TrainingType.RIGHT_LATEROTRUSION]

trainingDuration =5.0

lowerincisor =find("models/jawmodel/frameMarkers/lowerincisor")

for i in range(len(trainingList)):
    t =trainingList[i]
    m.setTrainingType(t)
    force_output_f ='data_files/force_' +t.getTrainingName() +'.txt'
    li_output_f ='data_files/li_' +t.getTrainingName() +'.txt'
    force_output =open(force_output_f, 'w')
    li_output =open(li_output_f, 'w')
    while getTime() <trainingDuration:
        force_output.write(m.getForce() +"\n")
        li_output.write(lowerincisor.getPosition().toString() +'\n')
        step()
    m.reset()
    reset()

```

```
force_output.close()
li_output.close()

quit()
```

A.3. Output probes

The following output probes were added to the jaw model in the class `artisyntn_models/.../dynjaw/JawDemo.java`.

A.3.1. Mouth opening distance

```
/* Mouth opening distance is calculated as inter-incisal distance. */
private class MouthOpeningDistance implements DataFunction{
    // eval is called every time step of the simulation
    public void eval(VectorNd vec, double t, double trel) {
        // calculate inter-incisal distance
        Point3d lower_incisor = ((FrameMarker)
            myJawModel.findComponent("frameMarkers/lowerincisor")).getPosition();
        Point3d upper_incisor = ((FrameMarker)
            myJawModel.findComponent("frameMarkers/upperincisor")).getPosition();

        double distance = new Vector3d().sub (lower_incisor,
            upper_incisor).norm ();
        vec.set (0, distance);
    }
}
```

A.3.2. Mouth opening angle

```
/* Mouth opening angle is calculated as the angle between the upper and
lower incisors in the saggital plane, in respect to the condylar centre
point. */
private class MouthOpeningAngle implements DataFunction{
    // eval is called every time step of the simulation
    public void eval(VectorNd vec, double t, double trel) {
        String[] components = {"ltmj", "rtmj", "lowerincisor",
            "upperincisor"};
        Point3d[] pts = new Point3d[4];
```

```

for(int i=0; i<components.length; i++){
    String c_name = components[i];
    pts[i] = ((FrameMarker)
        myJawModel.findComponent("frameMarkers/"+c_name)).getPosition();
}

Point3d condyleCentre = new Point3d();
condyleCentre.add(pts[0], pts[1]).scale (0.5); // condyle
        center = 0.5 * (ltmj + rtmj)
condyleCentre.set(0, 0); // project onto sagittal plane
pts[2].set (0, 0); // project lower and upper incisors onto
        sagittal plane
pts[3].set (0, 0);
Vector3d li = new Point3d().sub (pts[2], condyleCentre);
Vector3d ui = new Point3d().sub (pts[3], condyleCentre);

double angle = li.angle (ui);

vec.set (0, Math.toDegrees(angle));
}
}

```

A.4. FEM modelling of the articular disk

A.4.1. Code

The following code is from the file FEMDisk.java.

```

/* FEMDisk extends the jaw model with the articular disk in the TMJ */
public class FEMDisk extends JawDemo {

    FemModel3d disk;
    double diskWeight = 0.0006; // weight in kg (0.6g)

    // cylinder for making anterior ligament wrap around the condyle
    RigidBody cylinder;
    // lateral ligament
    MultiPointSpring llSpr;
    // medial ligament
    MultiPointSpring mlSpr;
    // anterior ligament
    MultiPointSpring alSpr = new MultiPointSpring();
    // posterior ligament

```

```

MultiPointSpring plSpr;
ArrayList<MultiPointSpring> springs = new ArrayList<>();

double[] maximumLengths = {2.5, 4, 1.9, 7.5}; // maximum extension of
    ligament lengths according to Sagl, 2019

// inc describes whether mouth opening muscle activation is currently
    incrementing
boolean inc = true;

public void build(String[] args) throws IOException {
    super.build(args);

    myJawModel.setIntegrator (Integrator.ConstrainedBackwardEuler);
    myJawModel.setMaxStepSize (0.001);

    // create and add FemModel
    disk = new FemModel3d ("disk");
    myJawModel.add (disk);

    PolygonalMesh condyleSurface = new PolygonalMesh("condyleSurface.obj");
    int layers = 4; // no. of layers
    double thickness = 0.2; // layer thickness
    double offset = 0.1; // centre the layers about the surface
    // create extrusion from condyle surface mesh
    FemFactory.createExtrusion( disk, layers, thickness, offset,
        condyleSurface );

    // set FEM material properties
    MooneyRivlinMaterial mat = new MooneyRivlinMaterial();
    mat.setC10 (9e5/1000); // convert Pa to mPa
    mat.setC01 (9e2/1000);
    disk.setStiffnessDamping (1.0);
    disk.setMaterial (mat);

    disk.setSurfaceRendering (SurfaceRender.Stress);

    disk.updateVolume ();
    double density = diskWeight / disk.getVolume ();
    disk.setDensity (density);

    // get jaw and maxilla position from jaw model
    RigidBody jaw = myJawModel.rigidBodies ().get ("jaw");
    RigidBody maxilla = myJawModel.rigidBodies ().get ("maxilla");
    RenderProps.setVisible (maxilla, true);

    myJawModel.setCollisionBehavior (disk, jaw, true);

```

```

// myJawModel.setCollisionBehavior (disk, maxilla, true);

Point3d ltmj_pos = myJawModel.frameMarkers ().get ("ltmj").getPosition
();
// the ltmj position (centre of left condyle) is used to position the
ligaments
double ltmj_x = ltmj_pos.x;
double ltmj_y = ltmj_pos.y;
double ltmj_z = ltmj_pos.z;

// create wrapping cylinder
cylinder = new RigidCylinder ("wrapSurface", /*rad=*/4, /*h=*/8,
/*density=*/0, /*nsegs=*/32);
cylinder.setPose (new RigidTransform3d(ltmj_x+4, ltmj_y, ltmj_z, 0, 90,
0));
myJawModel.addRigidBody (cylinder);
myJawModel.attachFrame (cylinder, jaw);
RenderProps.setVisible (cylinder, false);

// set rendering properties
setRenderProps ();

// add ligaments to hold disk in place
// for each ligament, a Particle is created for attaching one end of the
ligament to the jaw or maxilla
// a FemMarker is created for attaching the other end of the ligament to
the FEM disk

// Lateral Ligament (outside)
Particle l1 = new Particle("l1", .1, ltmj_x+8, ltmj_y, ltmj_z);
FemMarker l1Mkr = new FemMarker(ltmj_x+8, ltmj_y, ltmj_z+2);
l1Spr = addLigament(l1, jaw, l1Mkr);

// Medial Ligament (inside)
Particle m1 = new Particle("m1", .1, ltmj_x-8, ltmj_y, ltmj_z);
FemMarker m1Mkr = new FemMarker(ltmj_x-4, ltmj_y, ltmj_z+3.5);
m1Spr = addLigament(m1, jaw, m1Mkr);

// Anterior Ligament
Particle a1 = new Particle("a1", .1, ltmj_x+4, ltmj_y-4, ltmj_z);
FemMarker a1Mkr = new FemMarker(ltmj_x+4, ltmj_y-2.5, ltmj_z+3.5);
a1Spr = addLigament(a1, jaw, a1Mkr);

// Posterior Ligament
Particle p1 = new Particle("p1", .1, ltmj_x, ltmj_y+4, ltmj_z+6);
FemMarker p1Mkr = new FemMarker(ltmj_x, ltmj_y+4, ltmj_z+4);
p1Spr = addLigament(p1, maxilla, p1Mkr);

```

```

// add springs to a list
springs.add (l1Spr);
springs.add (a1Spr);
springs.add (m1Spr);
springs.add (p1Spr);
}

public MultiPointSpring addLigament(Particle p, RigidBody body, FemMarker
mkr) {

MultiPointMuscle spr = MultiPointMuscle.createLinear ();
LigamentAxialMaterial mat = new LigamentAxialMaterial();
mat.setDamping (0.005);
spr.setMaterial (mat);

myJawModel.addParticle(p);
myJawModel.attachPoint(p, body);
myJawModel.add (spr);
disk.addMarker (mkr);

// attach closest FEM nodes to FemMarker so that force of ligament will
// be distributed across several nodes
double attachmentRadius = 1.0;
ArrayList<FemNode3d> nodes = disk.findNearestNodes(mkr.getPosition (),
attachmentRadius);
mkr.setFromNodes (nodes);

spr.addPoint (p); // start of ligament is the particle attached to
maxilla/jaw

// in case of anterior ligament, add wrapping cylinder
if(p.getName ().equals ("a1")) {
spr.setSegmentWrappable (50);
spr.addPoint (mkr);
spr.addWrappable (cylinder);
spr.updateWrapSegments ();
} else {
spr.addPoint (mkr);
}

spr.setRestLengthFromPoints ();

return spr;
}

// This method is called every time step.

```

```

public StepAdjustment advance (double t0, double t1, int flags) {

    // check whether length of spring has reached maximum length
    // if so, increase elongation stiffness of the spring
    for(int i=0; i<4; i++) {
        MultiPointSpring spr = springs.get (i);
        if(spr.getLength () > spr.getRestLength() + maximumLengths[i]) {
            LigamentAxialMaterial mat = (LigamentAxialMaterial) spr.getMaterial
                ();
            mat.setElongStiffness (0.25);
        }
    }

    // perform opening movement
    Property excitation_property = myJawModel.getProperty
        ("exciters/bi_open:excitation");
    double openers_excitation = (double) excitation_property.get ();
    if(openers_excitation >= 0.15) {
        // stop incrementing opening muscle activation
        inc = false;
    }
    if(inc) {
        excitation_property.set (openers_excitation+0.005);
    } else if(openers_excitation > 0.005){
        excitation_property.set (openers_excitation-0.005);
    }

    return super.advance(t0, t1, flags);
}

```

A.4.2. Difficulties

In order to facilitate further attempts at modelling the articular disk, the encountered difficulties will be summarised in this section.

A dynamic simulation of the articular disk remains problematic because of the occurrence of inverted elements during the simulation. John Lloyd, principal software developer for ArtiSynth, explains this as follows:

“Inverted elements” occur when one or more elements deform to such an extent that their internal coordinate system is no longer right-handed, and has instead turned “inside-out”. An element’s initial position can also be inverted, if it is poorly constructed. Element inversion is a problem because the behavior of many nonlinear materials is not defined for an inverted coordinate system.

It is possible that using the `createExtrusion()` method from ArtiSynth resulted in some elements that are poorly formed and therefore “close” to being inverted. According to John Lloyd, this can happen when the extrusion occurs from a concave portion of the surface. However, the condyle surface is not concave, so it is not likely that this was a problem. Even so, in the ArtiSynth documentation it says that “for extrusions, no care is taken to ensure element quality; if the surface has a high curvature relative to the total extrusion thickness, then some elements will be inverted”.

Apart from this, there are many other factors influencing the occurrence of inverted elements. One factor is the choice of extrusion parameters, i.e. the number of layers of finite elements, the layer thickness and the offset of the FEM. The offset parameter does not describe a simple translation in z direction but a scaling of the mesh along the normal direction of the faces. The simulation was run several times with different values for the parameters, however it was inconclusive which parameters achieved the highest stability of the FEM. Nevertheless, it is important to note that if the offset is zero, inverted elements occur in the initial state because the FEM overlaps with the surface of the mandible.

This overlap also happens if the step size of the simulation is too high, i.e. with step size 0.01. The maximum step size should therefore be 0.001 and the most suited integrator was found to be the Backward Constrained Euler.

Another reason for inverted elements could be that the material for the FEM is not stiff enough to resist deformation properly, or that other material parameters, e.g. damping, are incorrect. “Getting the material parameters correct can be a bit tricky sometimes because they depend very much on the other units in your model (particularly mass and distance)” (John Lloyd).

Inverted elements can be visualised by exporting the mesh of the FEM to MeshLab, see Figure A.1. This shows where on the disk inverted elements occur and helps investigate their origin.

For the simulation, collision behaviour of FEM and mandible was enabled. A mouth opening movement during which the disk stays on top of the condyle is possible. However, the simulation is unstable when enabling collision behaviour with the maxilla. Without this collision, there is little to no stress acting on the disk, as it simply rests on the condyle and is pulled a little by the ligaments. Thus the stress cannot be evaluated.

Finally, it should be mentioned that the weight of the disk could not be represented properly. According to Sagl [25], the weight of the disk is 6 g. The disk is usually thinner towards the middle, where it lies flat on the condylar head, and is much thicker towards its border. When extruding from the surface mesh of the condyles, the FEM is equally thick everywhere and the overall volume will therefore be much less than the actual disk. In order to get the same density as in the model by Sagl [25], in the order of 10^{-6} , the weight of the disk was chosen to be 0.6 g, just $\frac{1}{10}$ of the original weight. This value has to be adjusted depending on the number of layers and layer thickness one uses for creating the extrusion.

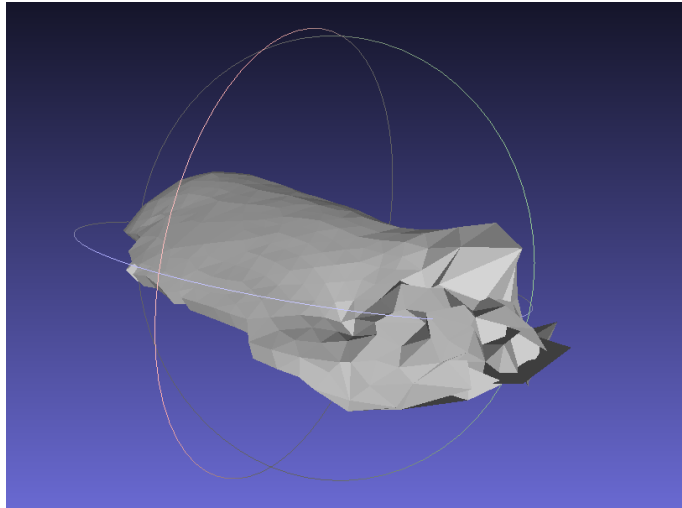


Figure A.1.: Inverted elements visualised in MeshLab.